

Ultrasonic Doppler Technique for Application to Multiphase Flows: A Review

Chao Tan^{1, 4#}, Yuichi Murai^{2#}, Weiling Liu^{1, 4}, Yuji Tasaka², Feng Dong¹, Yasushi Takeda³

¹Tianjin Key Laboratory of Process Measurement and Control, School of Electrical and Information Engineering, Tianjin University, Tianjin 300072, China

Email: tanchao@tju.edu.cn, liuweiling@tju.edu.cn, fdong@tju.edu.cn

²Laboratory for Flow Control, Faculty of Engineering, Hokkaido University, N13W8, Sapporo, Hokkaido, 060-8628, Japan

Email: murai@eng.hokudai.ac.jp, tasaka@eng.hokudai.ac.jp

³Food Process Engineering Laboratory, Swiss Federal Institute of Technology Zürich (ETHZ), LFO E 18, CH-8092, Zürich, Switzerland

Email: yasushi.takeda@hest.ethz.ch

⁴Key Laboratory of Efficient Utilization of Low and Medium Grade Energy, Ministry of Education, School of Electrical and Information Engineering, Tianjin University, Tianjin 300072, China

Abstract

Instantaneous velocity of multiphase flow is an important parameter in scientific and industrial applications such as fluid mechanics modeling and flow measurement and monitoring. Ultrasound Doppler provides the spatial-temporal distribution of multiphase flow velocity in a non-intrusive manner. This technique can be used to uncover the fluid dynamics by measuring the flow structures, detecting the gas–liquid interface position, measuring the multiphase rheology, and providing an online sensing solution for flowrate metering and flow status monitoring. These functions facilitate fluid dynamics investigations and modeling, industrial safety assurance and reliability, production estimation, and process control and optimization. This review focuses on the principle and the state-of-art development of the ultrasonic Doppler technique for measuring gas–liquid two-phase flow, liquid–liquid two-phase flow, and three-phase flow, and provides insights into the advantages, limitations, and future trends of this technique.

Keywords: Ultrasonic Doppler technique; Multiphase flow measurement; Flow velocity profile; Interface detection; Rheology measurement; Signal processing

1. Introduction

Multiphase flow exists in many industries such as food, bioengineering, chemical engineering, metallurgy, nuclear reactors, power plants, and petroleum. Typical multiphase flow includes solid–liquid, liquid–liquid, gas–liquid, and gas–solid two-phase flow, as well as gas–liquid–solid and gas–liquid–liquid three-phase flow ([Yan et al., 2018](#)). The spatial and temporal velocity distribution is necessary for understanding the behavioral and structural evolution of the flow and its heat or mass transfer, as well as to derive many flow parameters such as flowrate, turbulence intensity, and rheological parameters. These are important to fluid dynamics modeling, computation fluid dynamics (CFD) validation, and process monitoring and control ([Thorn et al., 2013](#)).

Many techniques for measuring flow velocity have been developed such as ultrasonic, electrical, and optical methods. Pressure/optical/electrical probes, including conductivity probes, optical probes, Pitot tubes,

These authors contributed equally to this work.

and hot wire anemometers (HWAs) usually obtain the local flow velocity at a single point (Lucas and Zhao, 2013; Prakash et al., 2019; Rusli et al., 2018). However, they are intrusive and disturb flows, which limits their applications. Another non-intrusive point-velocity measurement method is laser Doppler velocimetry (Kumara et al., 2010), which has high spatial and temporal resolution but needs precise optical alignment and fails in high-concentration or opaque fluids. Ultrasonic methods include the time-of-flight (ToF), cross-correlation, and Doppler methods. The ToF method suffers from blockage of the ultrasound path by the gas–liquid interface when the interfacial length scale is longer than the ultrasound pulse or beam width. The cross-correlation method requires careful design of the distance between two sets of transducers (one set upstream and the other downstream) and the data acquisition rate to compromise between the maximum detectable velocity and the similarity in signals from the two transducer sets. Based on echography and the Doppler effect, the non-intrusive ultrasonic Doppler technique can measure not only average velocity but also one-dimensional velocity profiles through pulse repetition emission (Takeda, 1986; Wongsaroj et al., 2020).

Because multiphase flow mostly shows multi-dimensional and time-changing fluid structures, its instantaneous two/three-dimensional velocity field (in a 2D plane or 3D space) needs to be captured (Tan et al., 2019). Therefore, techniques for measuring multi-dimensional multi-point velocity have emerged, such as the 2D electromagnetic method (Lehtikangas et al., 2016), 2D/3D particle imaging velocimetry (PIV) (Scarano, 2013), and 2D/3D X-ray tomography (Nabavi and Siddiqui, 2010). Each of their applications is limited by its measurement principle. For instance, the electromagnetic method is limited to conductive fluids, PIV requires dilute particle concentration and optical access to flow fields, and X-ray tomography requires careful radioactive protection. In contrast, the ultrasonic Doppler technique is radiation-free, compatible with opaque and aggressive fluids, and not limited by fluid conductivity. It can also obtain a 2D vector velocity profile using multiple transducers (Wongsaroj et al., 2020). General specifications of various velocity measurement instruments are summarized in Table 1.

Table 1. General specification of flow velocity measurement instruments

Measurement Instrument	Fluid phase distribution	Flow velocity	Spatial dimension	Spatial resolution	Velocity resolution	Sampling rate
Ultrasound Echo/Doppler	Echo	Doppler	1 to 2	0.3 to 1 mm	3 digits (8bit)	10 to 100 Hz
Optical Imaging (PIV, PTV, MTV)	Shadow/Reflection	PIV, PTV	2 to 3	Arbitrary lens optics	2 digits (5bit)	Arbitrary frame rate
X/Neutron Radiography	Attenuation	With PIV	1 to 2	1 to 10 mm	1 digit (3bit)	0.1 to 10 Hz
Electrical Tomography	Attenuation	With Time-lag	2 to 3	1 to 10 mm	1 digit (3bit)	10 to 100 Hz
Electric/Optical Probe	Binary signal	2-point correlation	0 (pointwise)	0.1 to 1 mm	3 digits (8bit)	1 kHz to 100 k Hz
Hot-Wire/Film Sensor	N.A.	Heat transfer rate	0 (pointwise)	1 to 5 mm	4 digits (12bit)	1 kHz to 100 kHz

The ultrasonic Doppler technique was first developed for inspecting cardiac function (Satomura, 1957) and blood flow with continuous waves (Franklin et al., 1961), and was further developed to measure the blood flow profile with pulsed ultrasonic waves (Satomura, 1959). In the 1970s, Baker proposed the physical principles and mathematical modeling of the pulsed ultrasonic Doppler method to measure one-dimensional

blood flow ([Baker, 1970](#)). Then, Brody introduced a stochastic multi-scattering model to estimate the average Doppler shift using the continuous-wave ultrasonic Doppler method ([Brody and Meindl, 1974](#)). In addition to being used in medicine ([Evans and McDicken, 2000](#)), Ultrasound Doppler was later applied in fluid mechanics through the pulsed-wave Doppler method ([Takeda, 1986](#); [Takeda, 1987](#)), and in fluid engineering for petroleum production logging ([Morriss and Hill, 1991](#)). Based on the pulsed ultrasonic Doppler method, the ultrasonic velocity profiler (UVP) has been developed to measure an instantaneous velocity profile ([Takeda, 1991](#)), and has been accepted and rapidly developed as an important measurement tool in fluid dynamics and engineering ([Kotze et al., 2013](#); [Ricci et al., 2017](#)).

Generally, the ultrasonic Doppler techniques for velocity measurement can be divided into the pulsed-wave ultrasonic Doppler (PWUD) ([Takeda, 1995](#)) and continuous-wave ultrasonic Doppler (CWUD) ([Dong et al., 2017](#); [Kouame et al., 2003a](#)) techniques. PWUD uses a single transducer to measure the velocity profile along a sound beam ([Takeda, 2012](#)), while CWUD uses two transducers to measure the average fluid velocity. They are both feasible for investigating multi-dimensional swirling flow, unsteady flow, turbulent flow, or transient flow by acquiring the two/three-dimensional velocity vector profile through multiple transducers ([Hurther and Lemmin, 1998](#); [Kikura et al., 2002](#); [Obayashi et al., 2008](#); [Rolland and Lemmin, 1997](#)). The piezoelectric ceramic transducer, linear array transducer, and phased-array transducer have been developed with special configurations to accurately visualize the velocity vector field for complex and transient flow structures ([Büttner et al., 2013](#); [Hamdani et al., 2016a](#); [Ricci et al., 2017](#)).

The ultrasonic Doppler technique is usually applied to gas–liquid and liquid–solid two-phase flow such as suspension flow and magnetic fluid flow ([Chemloul et al., 2009](#); [Dong et al., 2016a](#); [Turpeinen et al., 2020](#); [Wang et al., 2003](#); [Zhou et al., 1998](#)). Because the huge difference in acoustic impedance between gas and liquid induces strong reflection, the scattering ultrasound intensity and the signal-to-noise ratio (SNR) are high in gas–liquid two-phase flow. However, multi-scattering occurs when the particle concentration is high, which decreases the measurement accuracy. Therefore, most studies have focused on gas–liquid two-phase flow with a low void fraction rather than oil–water two-phase flow or oil–gas–water three-phase flow, where oil and water have a very small difference in acoustic impedance ([Dong et al., 2015](#); [Hitomi et al., 2017](#); [Tan et al., 2018](#)). The ultrasonic Doppler technique also helps in determining flow velocity profiles with single frequency ([Wongsaroj et al., 2019](#)) and multi-frequency (multi-wave) ultrasound ([Murakawa et al., 2005](#); [Nguyen et al., 2013b](#)), gas–liquid interface detection ([Coutinho et al., 2014](#); [Murai et al., 2006](#)), void fraction profiling ([Murai et al., 2009](#)), flow turbulence and structure characterization ([García et al., 2005](#); [Murakawa et al., 2003](#); [Shi et al., 2019](#)), and rheological evaluation ([Ricci et al., 2012](#); [Wiklund and Stading, 2008](#); [Yoshida et al., 2017](#)). Additionally, the ultrasonic Doppler signal can be combined with machine learning to use the flow velocity information in the frequency domain and phase fraction information in the time domain to identify flow regimes. This is more straightforward in revealing the flow conditions than using pressure/conductance/optical fluctuation signals ([Chakraborty and Das, 2020](#); [Shaban and Tavoularis, 2014](#)), and delivers an identification rate higher than 94% ([Abbagoni and Yeung, 2016](#); [Liu et al., 2021b](#); [Nnabuike et al., 2019](#); [Zhang et al., 2020](#)).

This review aims to give a comprehensive description of ultrasonic Doppler technology and its application in measuring gas–liquid and oil–water two-phase flow and three-phase flow, flow structure, and rheology with insight into its advantages and limitations in its sensing principle and processing algorithms. Recent research is discussed in detail, and future development and extensions of the ultrasonic Doppler technique are discussed. The review is organized as illustrated in **Fig. 1**. We begin with the fundamentals of the ultrasound Doppler method in Chapter 2, followed by its extension to multiphase flow measurement in Chapter 3. Because interfacial structure with different length scales matters for designing ultrasound signal

processing, we elaborate reported individual efforts in Chapter 3 before providing the summary and prospects in Chapter 4.

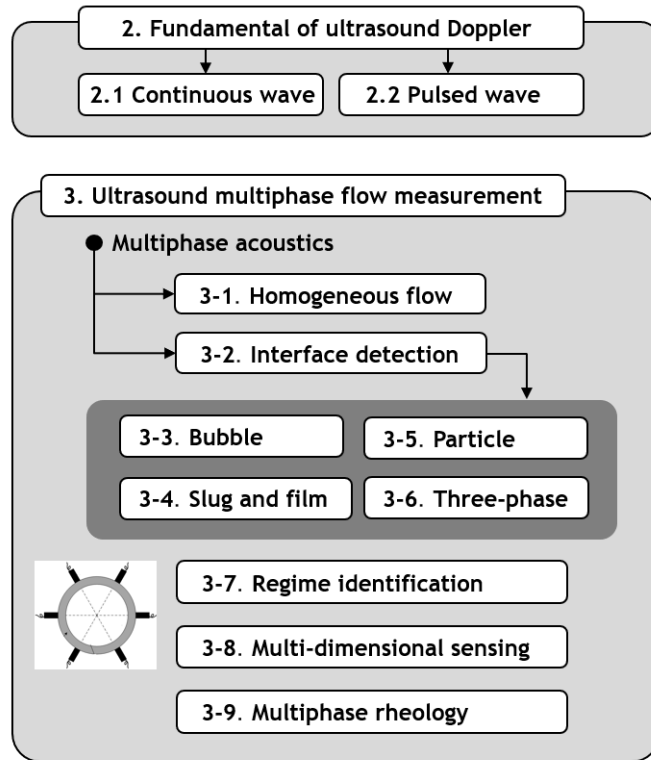


Fig. 1. Roadmap and section structure of this review.

2. Fundamental principle of the ultrasonic Doppler technique

The Doppler effect is named after Christian Andreas Doppler and states that when a sound source emitting a constant sound frequency is moving toward a receiver, the frequency of the received wave increases, and the frequency of the received waves decreases when the sound source moves away from the receiver. The ultrasonic Doppler technique measures the velocity of moving particles using the Doppler effect. The frequency difference, termed the Doppler shift frequency, is proportional to the relative velocity between the particle and the transducer. The CWUD and PWUD techniques both have their own advantages and limitations, which will be described next.

2.1 CWUD technique

CWUD adopts two transducers to continuously emit and receive ultrasonic waves. An example arrangement with transducers on opposite sides is described in **Fig. 2**. The sample volume is defined as the overlapping region of the transmitting and receiving ultrasonic beam paths located at the pipe center because the pipe diameter is usually larger than the beam width.

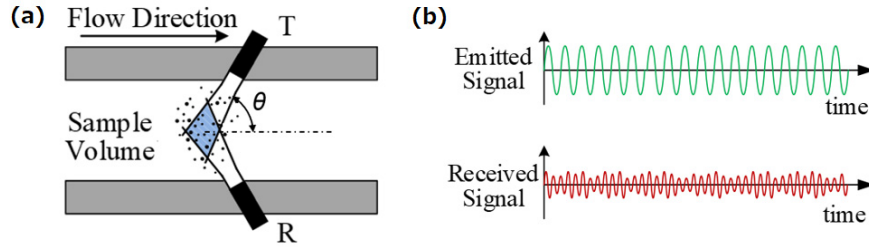


Fig. 2. Schematic of the CWUD principle: (a) CWUD sensors on opposite sides; (b) CWUD waveform.

Transducer T emits ultrasonic waves of frequency f_0 to the fluid, and transducer R receives the waves scattered by a particle in the sample volume (Baker and Yates, 1973). Owing to the relative motion between the particle and transducer T, the frequency f_1 of incident waves received by the particle is modulated according to the Doppler effect:

$$f_1 = \frac{c + u \cos \theta}{c} f_0, \quad (1)$$

where c is the speed of sound in fluid, u is the particle velocity in the main flow direction, and θ is the angle (Doppler angle) between the sound beam axis and particle flow direction. For the scattering waves, the moving particle is considered a secondary ultrasound source, and the relative motion between the particle and transducer R produces a second Doppler effect. Hence, the frequency f_r of scattering waves received by transducer R is also modulated by the relative motion between it and the particle, which can be expressed as

$$f_r = \frac{c}{c - u \cos \theta} f_1 = \left(1 + \frac{2u \cos \theta}{c - u \cos \theta} \right) f_0. \quad (2)$$

Because the flow velocity u is usually much lower than c , the term $(c - u \cos \theta)$ in Eq. (2) can be approximated as c , which simplifies frequency f_r to

$$f_r \approx \left(1 + \frac{2u \cos \theta}{c} \right) f_0. \quad (3)$$

As a result, the Doppler shift f_d can be calculated from

$$f_d = f_r - f_0 = \frac{2u \cos \theta}{c} f_0, \quad (4)$$

and the flow velocity u and velocity component v on the sound beam axis can be obtained via

$$u = \frac{c f_d}{2 f_0 \cos \theta}, \quad u_{beam} = u \cos \theta = \frac{c f_d}{2 f_0}. \quad (5)$$

The flow direction (forward flow or reverse flow) can be determined by detecting the polarity of the Doppler shift f_d of received echoes with respect to the emitted frequency f_0 .

Equation (4) shows that only the velocity component u_{beam} along the sound beam direction induces a Doppler effect. Therefore, when the particle's motion is perpendicular to the sound beam, a Doppler angle of $\theta = \pi/2$ leads to $f_d = 0$, so no frequency shift can be detected by the receiving transducer. In multiphase flow such as oil-gas-water flow, the dispersed droplets and small bubbles are usually regarded as inherent

scatterers whose actual velocity can be directly measured using the ultrasonic Doppler technique. When the particle or dispersed phase has good flow traceability, the velocity of the fluid or continuous phase is obtained by assuming its velocity is equal to that of the particle; otherwise, the slippage between the dispersed phase and continuous phase should be considered (Dong et al., 2016a).

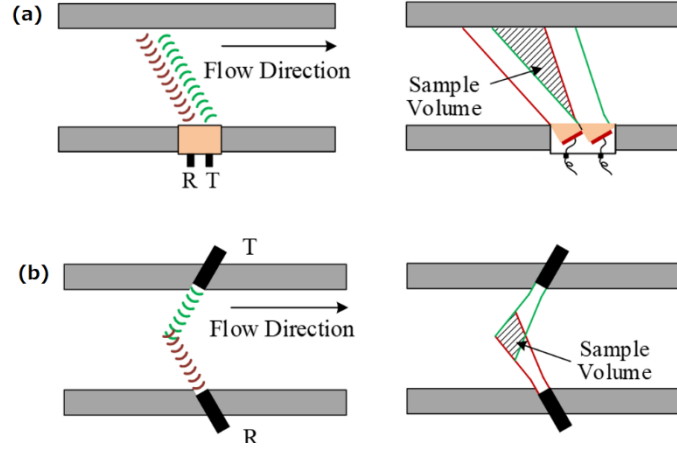


Fig. 3. CWUD sensor configurations and their sample volumes: (a) sensors on the same side; (b) sensors on opposite sides.

There are many randomly distributed scatterers moving through the sample volume. The echoes reflected by each scatterer are combined to form a composite Doppler shift, which is regarded as a weighted average of each scatterer's contribution. Therefore, the average Doppler velocity \bar{u}_{Dop} of scatterers is expressed as

$$\langle u_{Dop} \rangle = \frac{c \langle f_d \rangle}{2 f_0 \cos \theta}, \quad (6)$$

where $\langle f_d \rangle$ represents the average Doppler shift, whose power spectrum is a probability density function (PDF) of the Doppler signal in the frequency domain. The average Doppler shift can be evaluated using a weighted average power spectrum expressed as (Brody and Meindl, 1974)

$$\langle f_d \rangle = \frac{\int_{-\infty}^{+\infty} f \cdot S_d(f) df}{\int_{-\infty}^{+\infty} S_d(f) df}, \quad (7)$$

where $S_d(f)$ is the power spectrum of the Doppler shift, and f is the frequency component calculated through a fast Fourier transform (FFT). Owing to its continuous signal acquisition, CWUD has a high frequency resolution without limit on the maximum detectable velocity. However, CWUD has a fixed sample volume, so it is not possible to extract the Doppler shift from a local region of interest, and hence it does not have spatial resolution. The position and size of the sample volume directly affects the average velocity calculation because the Doppler shift is produced by the cumulative Doppler effect of each scatterer in the sample volume. In light of this, the sample volume of CWUD can be adjusted by arranging the transducers on the same side or on opposite sides, as shown in **Fig. 3**.

2.2 PWUD technique

PWUD adopts one transducer to emit and receive pulsed ultrasound waves, and uses ultrasonic echography and the instantaneous Doppler shift f_d of the echo signal to measure the velocity at a certain position along the sound beam path (measuring line). As shown in **Fig. 4(a)**, a transducer is set at an angle θ to the flow direction. It emits a short ultrasonic pulse with a basic frequency f_0 and then receives the echo from moving particles before emitting the next pulse. The measurement position x from which the pulse is reflected by particles can be located using the time delay Δt for the round trip between the transducer and the measurement position together with the speed of sound in fluid:

$$x = \frac{1}{2} c \Delta t . \quad (8)$$

The particle's velocity component v along the measuring line at measurement position x can be determined from the instantaneous Doppler shift f_d of the echo signal at the corresponding time. A series of discrete measurement channels along the sound path are established by changing Δt . Accordingly, the velocity distribution $v(x)$ can be obtained from f_d at each position. Therefore, PWUD can also be used to measure external flows such as a boundary layer flow, as shown in **Fig. 4(b)**.

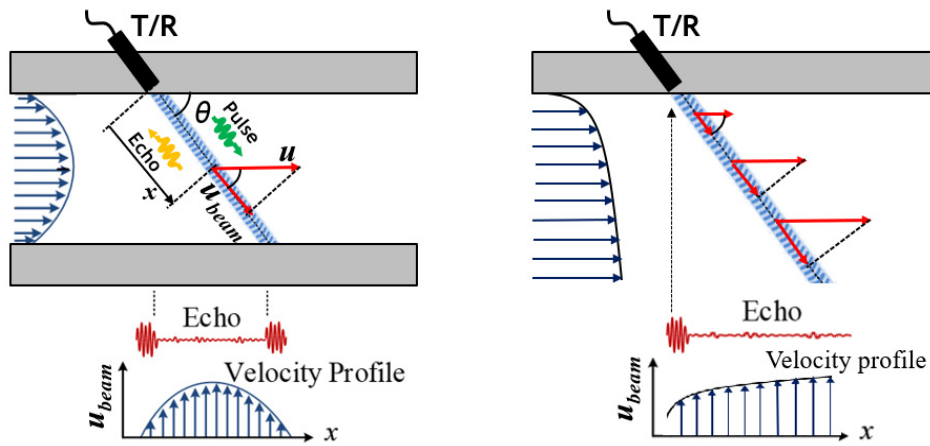


Fig. 4. Schematic of the PWUD principle: transducer configuration, echo signal, and reconstructed velocity profile for an (a) internal flow and (b) external flow. The symbol u_{beam} means the velocity component along the ultrasound beam.

Theoretically, there are various signal processing methods to derive the instantaneous Doppler shift f_d from the echo signal. However, because f_d is usually much lower than the frequency f_0 of the incident pulse (carrier frequency), and the pulse width is limited by the spatial resolution, it is difficult to extract f_d with high resolution from a single echo signal of one emitted pulse. Therefore, the ultrasonic pulse repetition Doppler method (UDM), involving repetition of pulse emissions and echo receptions, was developed to overcome this problem. As illustrated in **Fig. 5**, ultrasonic pulses are repeatedly emitted at a pulse repetition frequency (PRF) f_{prf} along the measuring line, and the collected echo signals are demodulated to extract the Doppler shift f_d from the carrier wave. Generally, each echo signal is preprocessed through quadrature phase demodulation, that is, multiplied by a cosine and a sine component and then filtered through a low-pass filter to eliminate the carrier wave frequency, as shown in **Fig. 6**. Each demodulated signal is resampled at the same delay time (shown by the dotted line in **Fig. 5**), which is related to a certain position along the measuring line. The resampled data then constitute a new signal called the Doppler signal, which carries the

Doppler shift frequency produced by the moving droplets in the corresponding sample volume. The Doppler shift f_d can be derived using various algorithms (such as an FFT or autocorrelation algorithm), and then the local Doppler velocity is obtained. The velocity profile along the measuring line is formed by repeating the above signal processing procedure at different measurement positions. This way, the sampling frequency of the Doppler signal at each position becomes the pulse repetition frequency f_{prf} .

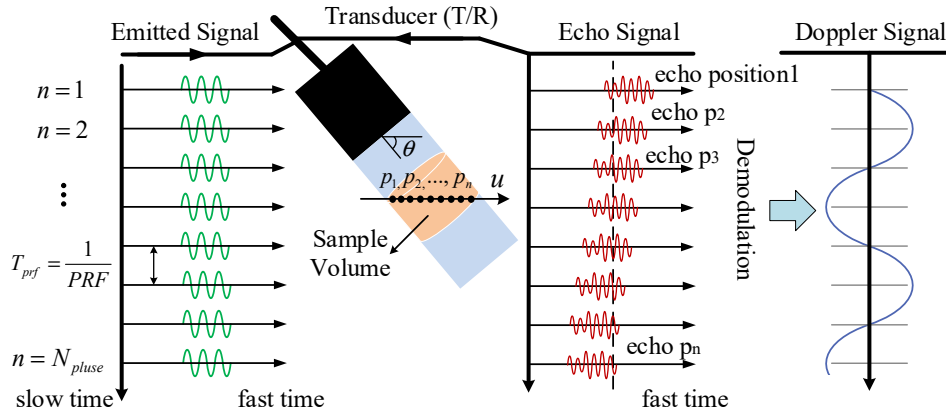


Fig. 5. Ultrasonic Doppler signal demodulation with the UDM.

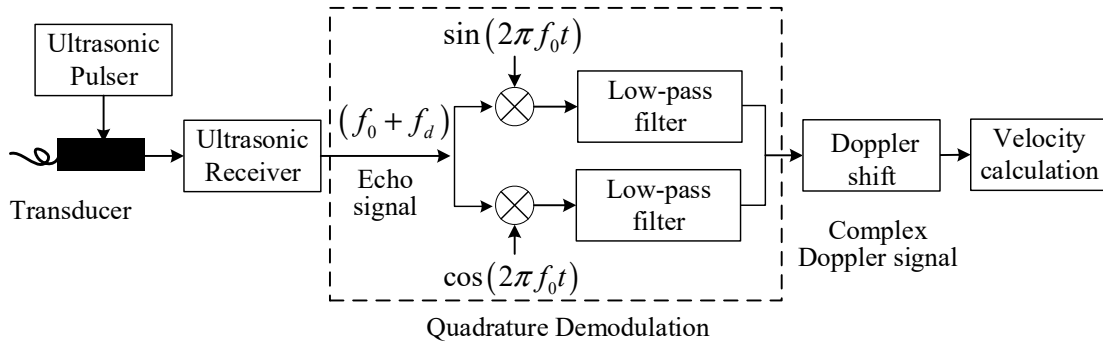


Fig. 6. Schematic of quadrature demodulation of an echo signal.

The spatial, temporal, temporal-frequency, and velocity resolutions of the conventional PWUD technique based on UDM are

$$\begin{cases} \Delta p = \frac{\lambda_0}{2} N_{cycle} = \frac{c}{2f_0} N_{cycle}, & \Delta t = N_{pulse} T_{prf}, \\ \Delta f_d = \frac{f_{prf}}{N_{pulse}}, & \Delta u_d = \frac{c \cdot \Delta f_d}{2f_0 \cos \theta}. \end{cases} \quad (9)$$

The spatial resolution Δp depends on half the ultrasonic pulse width, where N_{cycle} is the number of emitted pulse cycles (normally 4 to 8 cycles), and λ_0 is the wavelength. The time resolution Δt is the time interval between each velocity profile, where N_{pulse} is the number of pulse repetitions. The frequency resolution Δf_d is related to the sampling frequency f_{prf} of the Doppler signal and sampling number N_{pulse} . Therefore, the velocity resolution Δu_d is calculated from Δf_d . Because the Doppler signal of each measurement channel is

periodically sampled by the repeated echo signals, the maximum detectable Doppler shift $f_{d\max}$ of PWUD is limited to half the sampling frequency according to Nyquist theory: $f_{d\max} = 1/2 f_{prf}$. As a result, the maximum detectable velocity u_{\max} is

$$u_{\max} = \frac{c \cdot f_{prf}}{4 f_0 \cos \theta}. \quad (10)$$

If the measured velocity is higher than the maximum velocity, aliasing will appear and need to be compensated by post-processing the results or de-aliasing (Franca and Lemmin, 2006; Murakawa et al., 2015). As shown in Fig. 5., the sample volume of PWUD is a cylinder with an ultrasonic beam diameter and a thickness (length) of spatial resolution Δp . In practice, the diameter of each sample volume expands along the beam path owing to the ultrasonic beam divergence.

The maximum detected distance p_{\max} is determined by the pulse repetition interval (PRI) T_{prf} ($1/f_{prf}$) according to

$$p_{\max} = \frac{c}{2} T_{prf} = \frac{c}{2 f_{prf}}, \quad (11)$$

where T_{prf} is generally selected as the back-and-forth time of a pulse traveling between the transducer and the far-end wall to avoid pulse overlap. However, u_{\max} and p_{\max} are mutually constrained at the fixed f_0 according to

$$u_{\max} \cdot p_{\max} = \frac{c^2}{8 f_0 \cos \theta}. \quad (12)$$

If the maximum flow velocity is high, T_{prf} should be short to form a short detectable distance, and vice versa.

3. Multiphase flow measurement with the ultrasonic Doppler technique

The ultrasonic Doppler technique uses ultrasound transmission, reflection, and scattering in multiphase flow to measure the phase interface, dispersed phase size, volume fraction, flow velocity, or flow rate. The structure of multiphase flow can be roughly grouped into stratified flow and dispersed flow, which requires different set-ups of the ultrasonic transducers and sensing mode, as shown in Fig. 7. CWUD evaluates acoustic attenuation for dispersed flow, and blockage by stratified flow between two transducers. PWUD obtains pulse reflections from the interfaces in the flow. When a gas phase exists in the upper part of the pipe in stratified flows, a bottom-up transducer arrangement can capture plug flows, slug flows, and wavy flows (Gonzalez A et al., 2009). Non-axisymmetric multiphase flow structures under different flow patterns require multi-line transducer arrangements, as shown in Fig. 8.

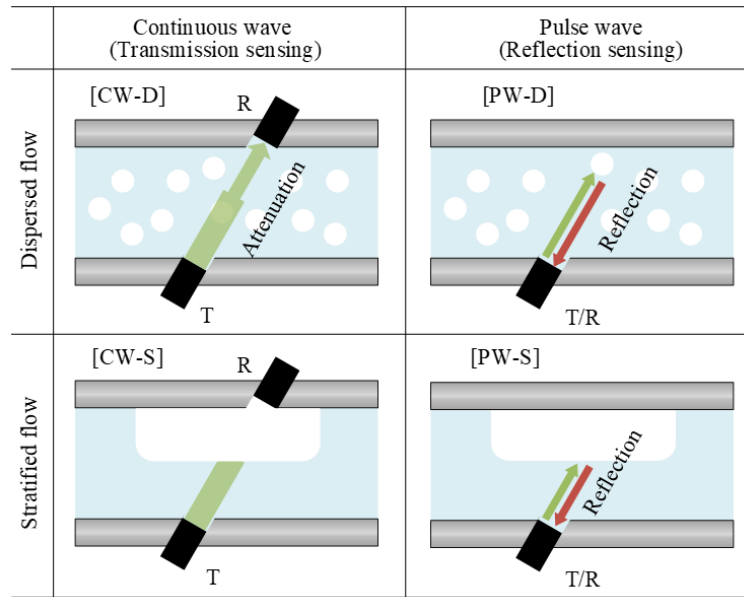


Fig. 7. Basic classification of ultrasonic sensing for multiphase flows.

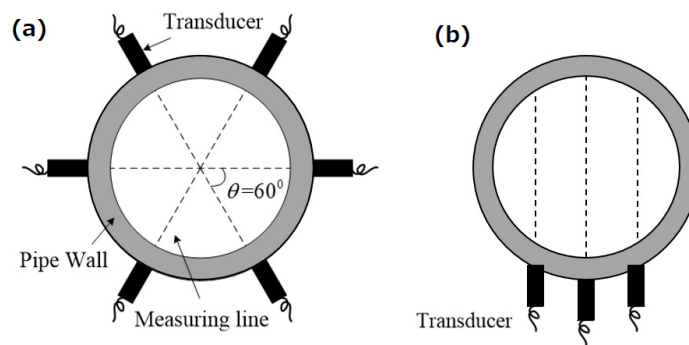


Fig. 8. Multi-line transducer arrangements for pipe flow: (a) angular arrangement for dispersed multiphase flows; (b) vertical parallel arrangement for stratified multiphase flows.

In multiphase flow, the adopted signal processing scheme relies on the characteristic length scale L of the interface relative to the ultrasound wavelength λ . Note that λ is on the sub-millimeter order in most kinds of liquid for the commonly used ultrasound basic frequency range $f_0=1$ MHz to 4 MHz. **Table 2** possible quantities of multiphase flow to be measured via ultrasound when liquid constitutes the carrier phase. For $L > \lambda$, the interfacial profile and turbulence properties are the main measurement targets in separate/stratified flow, while in homogenous flow, the flow rate and rheological properties are the quantities of interest. On a comparable scale at $L \sim \lambda$, the dispersion distribution causes two-phase flow to exhibit various behaviors such as slippage between two phases and distributed density, which are all desirable for measurement. To this end, multiple quantities can be extracted from ultrasound echoes such as attenuation, change in speed of sound, frequency shift, and waveform distortion, which can be jointly used for measurement. However, it is not easy for other instruments to measure multiple quantities simultaneously. Such a scheme is often achieved by combining multiple sensors such as pressure sensors and electrical sensors.

Table 2. Target measurement quantities in multiphase flows where liquid is carrier phase

Interfacial length		$L > \lambda$	$L \sim \lambda$	$L < \lambda$
Added phase	Mixing of gas	Plug/slug flow	Bubbly/film flow	Microbubbles
	Mixing of liquid	Stratified flow	Droplet flow	Emulsion
	Mixing of solid	External flow	Granular flow	Suspension
Quantity to be measured	Volume flow rate	√	√	√
	Volume fraction	√	√	√
	Interfacial profile	√	√	
	Dispersion profile		√	
	Dispersion size		√	
	Turbulence property	√	√	
	Rheological property		√	√

In any set-up and for any target, the speed of sound in multiphase flow is a crucial property that needs to be correctly determined to use Ultrasound Doppler technique. When multiphase flow comprises liquid and solid only, the speed of sound is simply estimated from the average bulk modulus and mixture density. When bubbles are involved in the flow, the gas phase compressibility significantly reduces the speed of sound. For low-frequency acoustic waves, the speed of sound in bubbly liquid is given by

$$c = \sqrt{\frac{d\rho}{d\phi}} = \sqrt{\frac{p/\rho_L}{\alpha_G(1-\alpha_G)}}, \quad \rho = \rho_L(1-\alpha_G), \quad (13)$$

where α_L , p , and α_G are the liquid density, pressure, and gas volume fraction respectively. For example, the speed decreases to $c=30$ m/s for atmospheric pressure at $\alpha_G = 50\%$, much slower than the speed of sound in air. **Fig. 9** presents the speed of sound in bubbly liquid changing with sound frequency f (Ando et al., 2011). The abscissa is normalized by the bubble’s volumetric resonant frequency (Plesset and Prosperetti, 1977) given by

$$f_{resonant} = \frac{1}{\pi d} \sqrt{\frac{1}{\rho} \left(3p + \frac{8\sigma}{d} \right)}, \quad (14)$$

where p is the ambient pressure and σ the surface tension. When $f/f_{resonant}$ is around unity, the speed sharply depends on the sound frequency as well as on the deviation in bubble size. This occurs owing to the bubble’s volumetric pulsation excited by resonance and the complicated propagation of pressure waves through bubbly media. Note that the data in **Fig. 9** are for a mean bubble size of 20 μm . For mm-sized bubbles, the trend is theoretically the same for the frequency normalized by the resonance frequency if bubble deformation and clustering are assumed to be insignificant. In contrast, most ultrasonic waves have a frequency sufficiently higher than the resonant frequency, which ranges from 100 Hz to 300 kHz depending on bubble size. Thus, the speed of sound is kept nearly the same as in the liquid phase. This allows ultrasonic echography and the Doppler technique to be carried out using the speed of sound in liquid even for bubbly liquids.

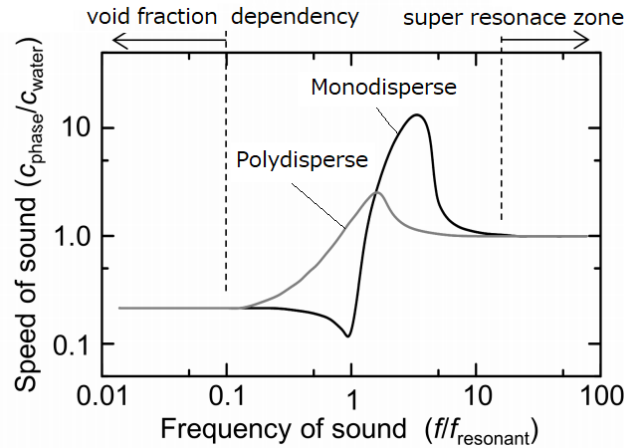


Fig. 9. Speed of sound in bubbly liquid relative to that in water varying with sound frequency, as analyzed by [Ando et al. \(2011\)](#), where f_{resonant} stands for the resonant frequency of the bubble's volumetric pulsation. The bubble size is around $20 \mu\text{m}$ when $f_{\text{resonant}}=0.29 \text{ MHz}$ for a gas volume fraction of 0.1%. The graph is slightly expanded by the authors to explain plateau zones on both sides.

3.1 Homogeneous multiphase flow measurement

Homogeneous multiphase flow has no inter-phase slippage and thus has one velocity field, such as emulsion or particle suspension flow. The main challenges with such flows are the difficulty in realizing non-intrusive and online monitoring of the flow rate (flow metering) and the rheological influence on the spatial or temporal development of the flow in different flow geometries when optical access is limited by fluid opaqueness.

Ultrasonic flowmeters have a long history of technical development to deal with such challenges ([Lynnworth and Liu, 2006](#); [Muramatsu et al., 2018](#)), and Ultrasound Doppler shows the highest flexibility and reliability in adapting to different multiphase flows. In the history of single-phase ultrasonic flow-metering, CWUD has been used to capture the mean velocity in given flow geometries, typically in pipes. In particular, the velocity measured with CWUD sensors on opposite sides is not disturbed by vertical motion of scatterers, because the positive contribution of this motion to the transmitting transducer can be cancelled by its negative contribution to the receiving transducer ([Kouame et al., 2003a](#)). CWUD has a fixed sample volume, and the measured Doppler shift only depends on the axial velocity of scatterers. The accuracy can be increased through a high-resolution frequency technique based on reassignment or parametric modeling that eliminates the colored noise of a Doppler signal ([Kouame et al., 2003b](#)). Therefore, CWUD is appropriate for estimating the average flowrate. For non-ideal flow conditions such as a non-developed turbulent flow, swirl flow at a bend, or a sudden expansion in a pipe, the velocity distribution is non-axisymmetric. Hence, multi-line measurement is used to reduce the measurement error ([Treenuson et al., 2013](#); [Wada et al., 2004](#)), as shown in **Fig. 8**. By regarding the multi-line velocity profiles along the circumferential measuring circle as a kind of wave, one can use the Nyquist sampling theorem to estimate the optimal number of transducers for accurate flowrate measurement, which is just twice the wave number of the velocity profile along the measuring circle ([Treenuson et al., 2013](#)).

Although the echo intensity from an oil–water interface is much lower than from gas–liquid interfaces owing to the similar acoustic impedances of oil and water, the echo signal is still detectable for calculating the flow velocity in the full range of the phase fraction. In oil–water flow, the dispersed oil or water droplets are the natural scatterers for reflecting ultrasonic waves, and the averaged Doppler shift over the pipe cross-section is nonlinearly proportional to the phase velocities ([Morris and Hill, 1991](#)). The results are

affected by the multiple reflections near the transducer and the change in sound speed of a fluid mixture caused by the change in phase fraction. The beam spreading and the insufficient echo intensity reflected from very fine liquid droplets at low concentration (<10%) also decrease the measurement accuracy (Mahadeva et al., 2010). Therefore, to improve the echo intensity and alleviate the influence of sound speed change on Doppler measurement, a high-power CWUD system with sensors on opposite sides was built and a new mathematical Doppler model for separated flow was established with an equivalent sound speed (Dong et al., 2015). Because oil and water have similar densities and dynamic viscosities, the average ultrasonic Doppler shift $\langle f_d \rangle$ is proportional to the overall superficial velocity on two slopes, which correspond to the water-continuous and oil-continuous flows (Dong et al., 2015), as shown in Fig. 10. Therefore, effective models are required to correlate f_d with flow velocity to cope with the complex flow velocity distribution. A measurement model based on the power-law velocity profiles of dispersed flow was developed to relate the average velocity of a dispersed phase (i.e., the measured Doppler velocity) within the sample volume to the overall superficial velocity, delivering a measurement error of 3.63% for overall superficial velocity. The measurement error was further reduced to 2.27% by introducing the drift-flux model into the previous model. The drift-flux model can describe the theoretical correlation between the superficial velocity and dispersed phase velocity on the basis of slippage between two phases (Dong et al., 2016b). When ultrasound propagates in the layers of oil and water, the velocity profile in each layer should be separately considered. A boundary layer model for dispersed flow and stratified flow was presented for such applications with a measurement error of 2.8% for the overall superficial velocity (Tan et al., 2016), which is comparable to or even smaller than that for conventional cross-correlation with a capacitance/conductance probe or the differential pressure method, whose average error is below 5% (Tan et al., 2013; Zhai et al., 2014). Experiments indicate that the average Doppler shift of CWUD with sensors on the same side is similar to that of CWUD with sensors on opposite sides. Therefore, the overall superficial velocity can be derived from a linear correction of $\langle f_d \rangle$ for continuous oil and water flows (Liu et al., 2018).

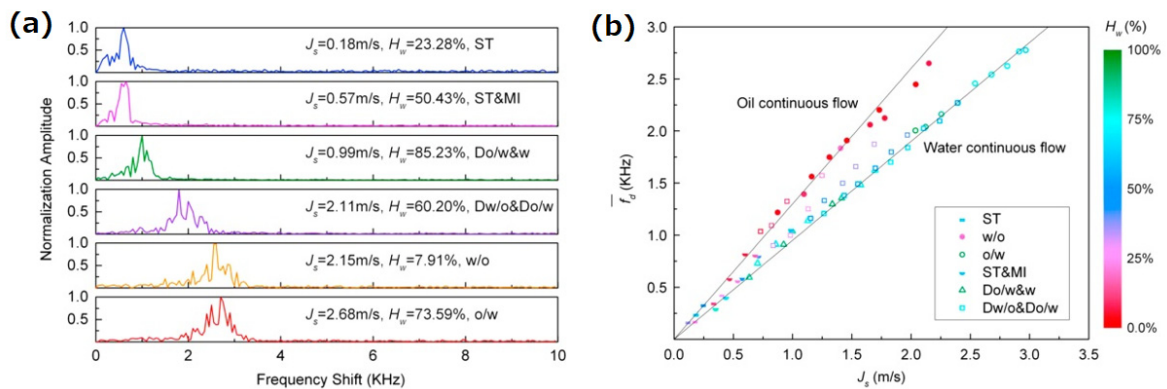


Fig. 10. Oil–water two-phase flow measurement: (a) average Doppler spectrum; (b) dual-slope relations with superficial velocity (Dong et al., 2015).

The accuracy of a velocity profile of oil–water two-phase flow measured via PWUD was verified with laser Doppler velocimetry data under similar flow conditions (Dong et al., 2019). The velocity profiles of different flow patterns could be fitted into a boundary layer model to form a dual-slope distribution for continuous water and oil flows, as shown in Fig. 11 and Fig. 12. The form of the boundary model is

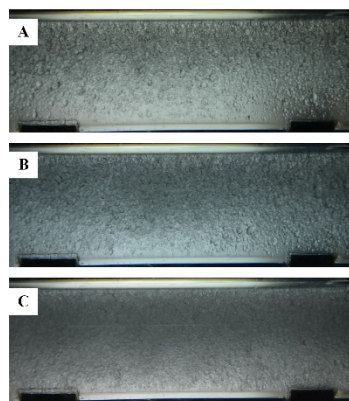
$$u^+ = k \ln y^+ + B, \quad (15)$$

where k and B are the coefficients, and u^+ and y^+ are the dimensionless forms of the axial velocity u and distance y_w from the pipe wall:

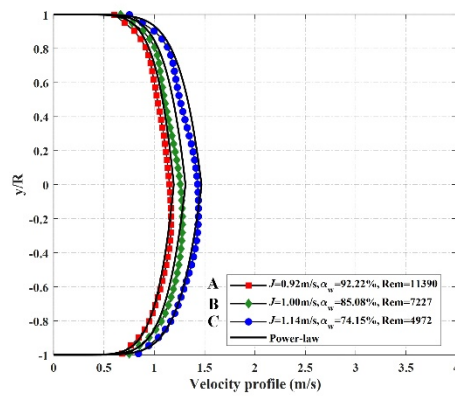
$$u^+ = \frac{u}{u_\tau}, \quad y^+ = \frac{y_w u_\tau}{\nu}, \quad (16)$$

where u_τ is the wall shear velocity and ν the kinematic viscosity.

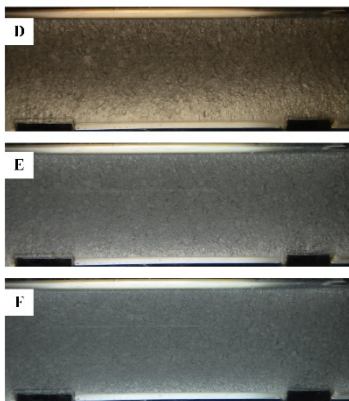
Therefore, the average velocity of the dispersed phase can be calculated by integrating the velocity profile and ignoring the slippage between the two phases. However, this method brings errors due to the interphase slippage. To mitigate this problem, the measured velocity profile can be substituted into the drift-flux model to correlate the velocity profile of the dispersed phase with the overall superficial velocity, in which the relative velocity is derived by analyzing the force on droplets (Liu et al., 2018). The error in overall superficial velocity caused by interphase slippage can be reduced by 60% and is mainly between -8% and 7%.



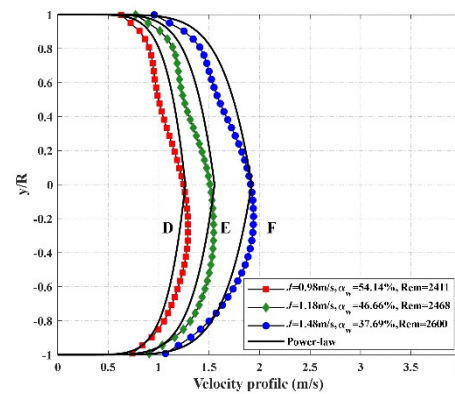
(a) Photos of Do/w&w flows



(b) Velocity profiles for (a)



(c) Photos of Dw/o&Do/w flows



(d) Velocity profiles for (c)

Fig. 11. Photos and measured velocity profiles of dispersed oil in water and water (Do/w&w) flows and dispersed water in oil and dispersed oil in water (Dw/o&Do/w) flows.

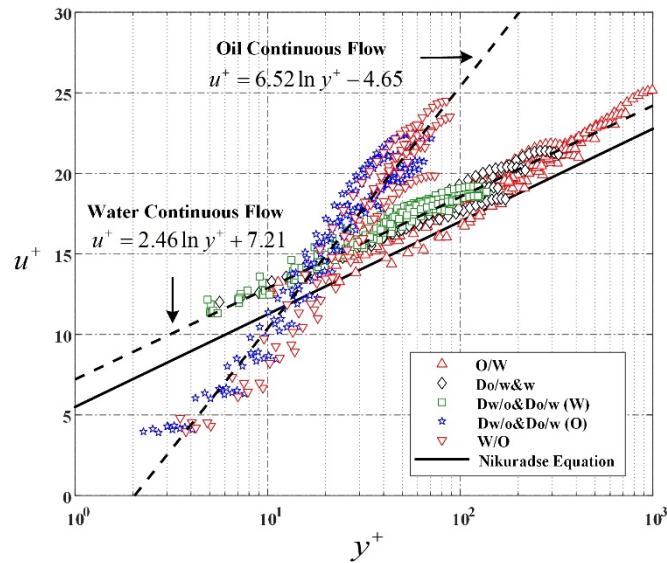


Fig. 12. Dimensionless velocity distribution of horizontal oil–water two-phase flow.

For fiber suspensions, which are assumed to be nearly homogenous two-phase flows, PWUD is immediately applicable to obtain flow velocity profiles. Claesson et al. (2013) measured the flow structures of a jet in a fiber suspension at variable concentration (Fig. 13) and found the momentum diffusion was lower than in Newtonian laminar flow. PWUD has been widely used to investigate non-Newtonian fluid flows such as polymer and emulsion flows. When these additives form interfaces and phase distributions on a length scale comparable to the characteristic scale of flow, a multiphase flow problem arises for which ultrasound needs to capture the interface in addition to the Doppler shift.

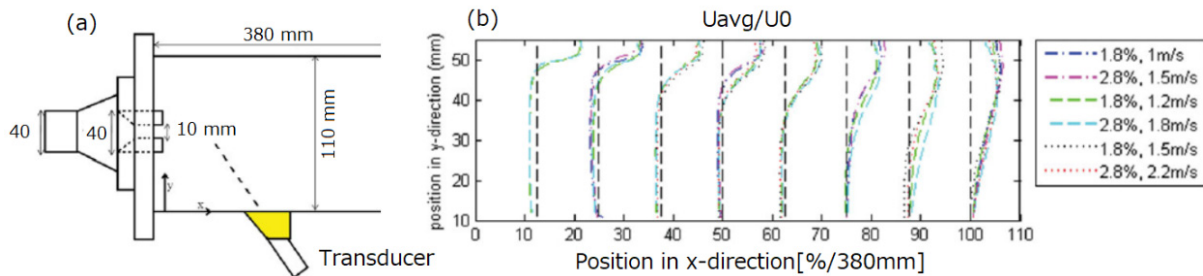


Fig. 13. Velocity profile of a fiber suspension measured by Claesson et al. (2013): (a) measurement set-up; (b) measured streamwise velocity profiles indicating the centerline velocity is sustained longer than Newtonian laminar flow.

3.2 Interface detection through ultrasound pulses

In multiphase flow, measuring the interface and volume fraction profile helps reveal the flow structure evolution and refine fluid models. When ultrasound propagates in multiphase flow, the reflection echo exhibits a complex amplitude and frequency that depend on the size, shape, and velocity of the interface, and on the acoustic impedance difference between phases. This leads to various signal processing algorithms in PWUD. There are two major approaches to detect the phase interface using ultrasonic reflection: the pulse-echo intensity method and local Doppler method. The position of the interface is obtained from the time of flight at which an echo or Doppler signal indicates the presence of the interface. In both cases, the characteristic length scale L of the interface relative to the ultrasound wavelength λ in the carrier liquid phase

determines the measurement principle.

Fig. 14 illustrates the ultrasound reflection patterns in gas–liquid two-phase flow. For spherical bubbles smaller than λ , the reflection wave obeys Rayleigh scattering, that is, the wave propagates in the radial direction of individual bubbles. Ultrasound produces diffused reflection on the interface when capillary waves are subject to $L < \lambda$. In contrast, ultrasound exhibits mirror reflection on a large bubble and a long, smooth, and free surface for $L > \lambda$. For bubbles with $L \sim \lambda$, heterogeneous reflection occurs as Mie scattering of light. **Table 3** summarizes how the ultrasonic reflection wave is used to detect the interfaces in a flow. The information is often unavailable for a high-void-fraction two-phase flow owing to the limited acoustic transmission over a gas–liquid interface. Hence, either one of the available signals or their combination is used (Murai et al., 2010).

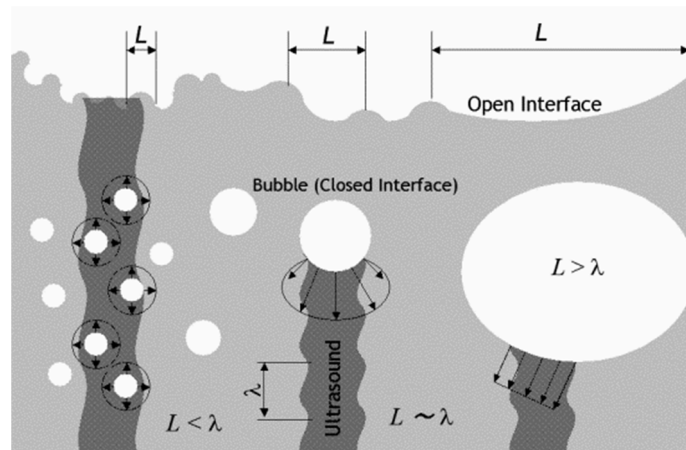


Fig. 14. Ultrasound reflection around various interfaces with a characteristic length scale L relative to the ultrasound wavelength in a carrier liquid phase (Murai et al., 2010).

Table 3. Classification of ultrasound detection of gas-liquid interfaces

Information detected from reflection wave of ultrasound pulse	Length scale of interface L , relative to basic wavelength of ultrasound λ		
	$L > \lambda$	$L \sim \lambda$	$L < \lambda$
Time of flight (Phase of wave)	Phase is conserved for closed interface like a bubble, and is reversed for opened interface.	Phase depends on surface tension (or rigidity of interface).	Phase is reversed due to kinematical free boundary.
Echo intensity (Amplitude)	Being weakened by diffused reflection.	Heterogenous reflection due to interference.	Being kept with mirror reflection.
Doppler velocity (Frequency)	Moving velocity of interface modifies the frequency of reflection wave.	Moving velocity of interface modifies the frequency of reflection wave.	Significant Layer of local standing wave is generated to erase Doppler shift.

3.2.1 Interface detection with ultrasonic pulse echo intensity

For the pulse-echo intensity method, the interface is detected from the pulse-echo amplitude reflected from the interface (Duffey and Hall, 1969), because a large difference in acoustic impedance at the interface causes a high reflection intensity. By capturing the echoes with an amplitude higher than a threshold, one can locate the gas–liquid interface by calculating the time of flight of the captured echoes traveling between the

transducer and the interface. This method is easily applied to large interfaces, for instance, the horizontal slug flow measurement shown in **Fig. 15**. A sharp and clear echo intensity is reflected from the interface while the Doppler shift shows a continuous flow profile inside the liquid phase ([Murai et al., 2009](#)). The void fraction can be estimated from the echo intensity in a vertical two-phase flow with a statistically axisymmetric gas phase distribution ([Na et al., 2021](#)).

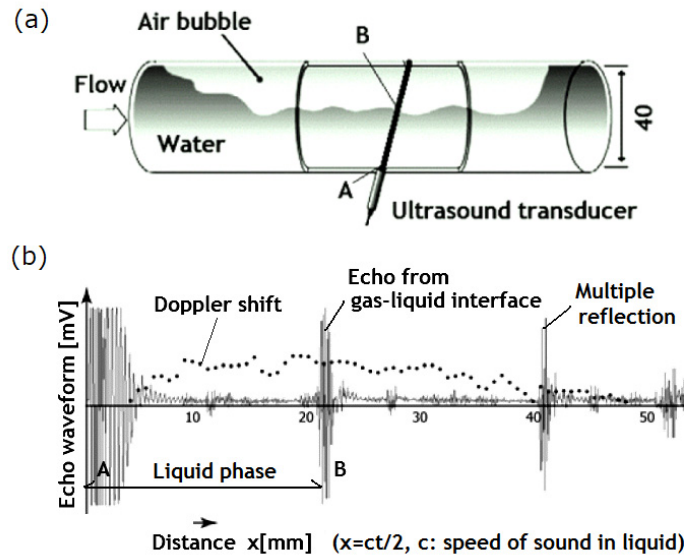


Fig. 15. Horizontal gas–liquid slug flow measurement ([Murai et al., 2009](#)): (a) set-up; (b) instantaneous echo intensity profiles (line) and Doppler shift (dots) along the measurement line.

The echo intensity can also be used to measure liquid film thickness ([Park and Chun, 1985](#)) and detect the interface motion of different flow patterns in horizontal gas–water two-phase flow ([Chang and Morala, 1990](#); [Matikainen et al., 1986](#); [Wada et al., 2006](#)). The velocity, bubble length, and liquid film thickness of Taylor bubbles in a vertical or inclined pipe can be measured by treating the bubble boundary as an interface ([de Azevedo et al., 2020](#); [de Azevedo et al., 2017](#); [Murakawa et al., 2008](#)). Individual bubbles flowing faster than 3 m/s near a wall can be captured by increasing the data sampling rate, as shown in **Fig. 16**. It has been proved that bubbles always leave a liquid film with a thickness comparable to the buffer layer thickness in the turbulent boundary layer. The same approach is used to measure the film thickness of liquid flowing along a wall in a gaseous ambience ([Al-Aufi et al., 2019](#)), as shown in **Fig. 17**. As long as the acoustic property of the layers between the transducer and the liquid is known, the interface position can be analytically extracted from the overlapped waveform.

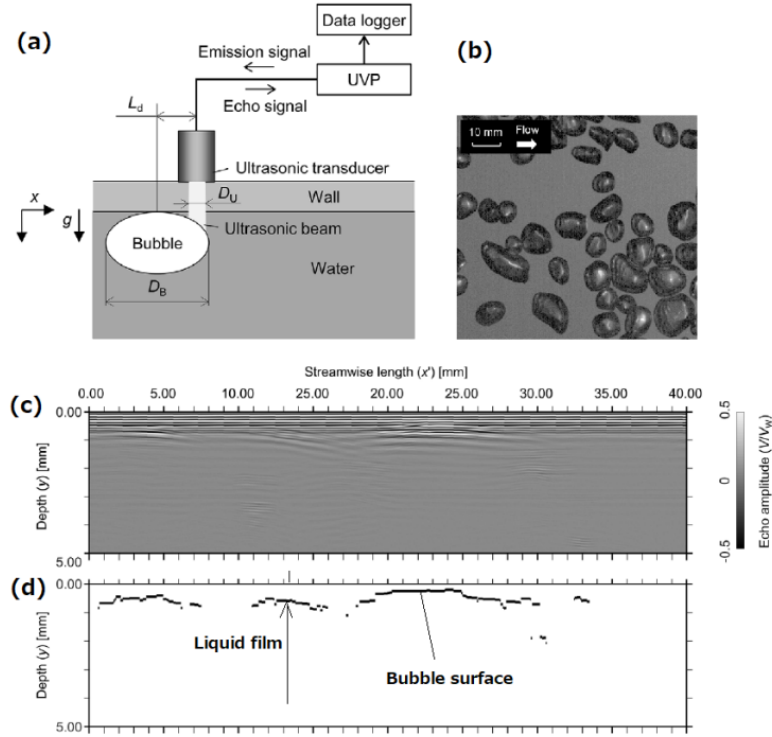


Fig. 16. Bubble surface and liquid film thickness measured via pulsed-wave ultrasound high-resolution echography (Park et al., 2015): (a) set-up; (b) upper view of bubbles; (c) obtained echo waveform blown up in time; (d) detected bubble interface.

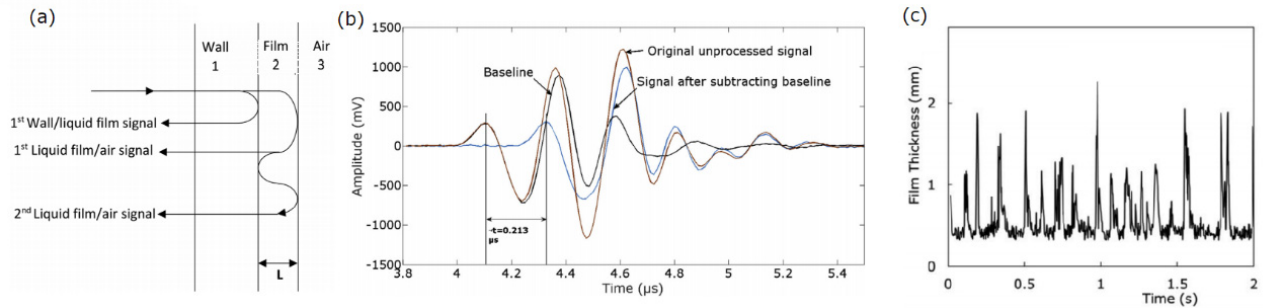


Fig. 17. Liquid film thickness measurement by Al-Aufi et al. (2019): (a) diagram of expected ultrasound path; (b) ultrasound signal deforming from the baseline signal owing to the presence of a liquid film; (c) measured variation of the film thickness descending inside a 127-mm-diameter tube.

3.2.2 Interface detection with the ultrasonic pulse Doppler method

An alternative method to detect large interfaces with local Doppler shift signals is called the local-pulse Doppler method. As shown in Fig. 18, a standing wave layer is formed in the liquid phase near the bubble interface, caused by the overlap of incident and reflected waves during mirror reflection within half the pulse length from the interface (Longo, 2006). The particles within the standing wave layer do not produce a Doppler shift regardless of flow velocity. Hence, the local Doppler method can detect the interface by finding the zero-Doppler velocity layer along the PWUD measuring line, and the detection performance is not affected by the distance between the interface and transducer. This method has been used to detect the bubble interface in turbulent bubbly flow in a rectangular channel (Murai et al., 2006) and in a circular tube (Gonzalez

A et al., 2009). The zero-Doppler layer can be simply detected by examining space-time two-dimensional filtering of the Doppler shift distribution, as shown in Fig. 19. Among three kinds of 3×3 filters, the Sobel filter worked best for extracting the interface. The method was further experimentally verified for detecting a smooth interface larger than the ultrasonic beam diameter over a wide range of interface angles (Murai et al., 2010).

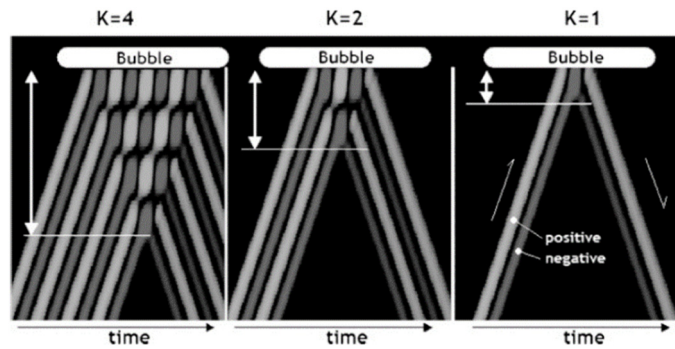


Fig. 18. Local standing waves formed near the gas–liquid interface in the space-time domain, canceling out the Doppler shift regardless of flow velocity (Murai et al., 2009); K stands for number of cycles in a pulse.

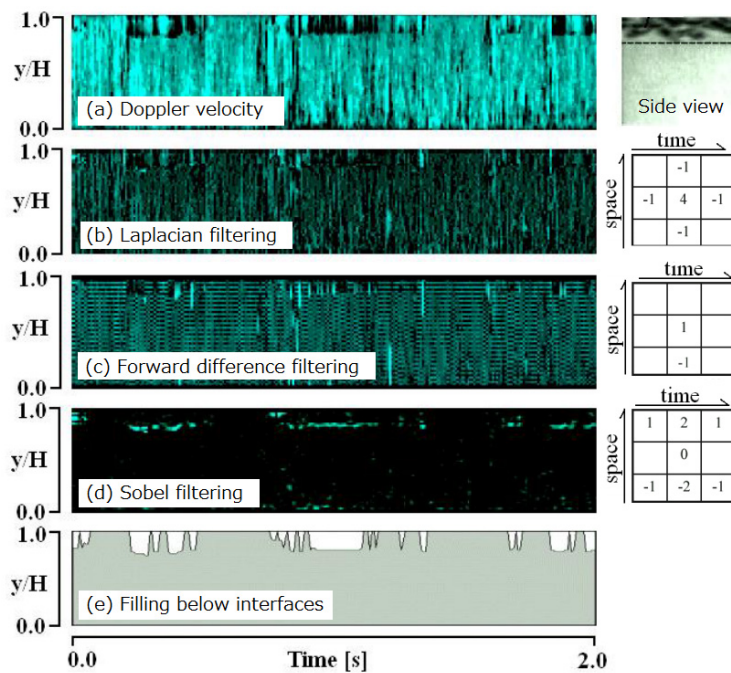


Fig. 19. Bubble detection in a horizontal turbulent channel flow from the Doppler velocity distribution for a flow speed of 1 m/s and channel height of 40 mm (Murai et al., 2006): comparison of three kinds of space-time 3×3 filters for detecting the interface from the Doppler signal.

3.3 Bubbly two-phase flow measurement

The huge acoustic impedance difference between gas and liquid causes a strong reflection of incident ultrasound at the interface. Because bubbles have a nearly massless dispersion, the non-intrusiveness of ultrasound measurement is suitable for measuring the bubble size (Morris and Hill, 1993), especially in opaque liquids such as chemical solutions, liquid fuels, cray/mud suspensions, and liquid metals (Wang et al.,

2003; Wang et al., 2017).

3.3.1 Bubble measurement

There is a very strong demand in industry for detecting bubbles and measuring the void fraction of gas–liquid two-phase flow. Ultrasonic tomography can reconstruct the phase distribution by measuring the ultrasound attenuation or time of flight through a set of transducers installed on the pipe wall (Tan et al., 2019). Fig. 20 shows examples of cross-sectional void fractions in a pipe measured by Supardan et al. (2007) with six pairs of ultrasound emitters and receivers attached around a pipe. They could evaluate how the bubble distribution was affected by a baffle inserted in an upward co-current bubbly flow. For flows containing microbubbles smaller than 200 μm , the microbubbles distort ultrasound echo waveforms in terms of the local amplitude and frequency of the pulse, which are estimated from acoustic theory. Park et al. (2021) succeeded in simultaneously measuring the microbubble diameter and void fraction in a narrow channel flow as a function of time (Fig. 21). The technique is applicable to fluid bearing with a risk of gas ventilation and to fluidic devices handling microbubbles.

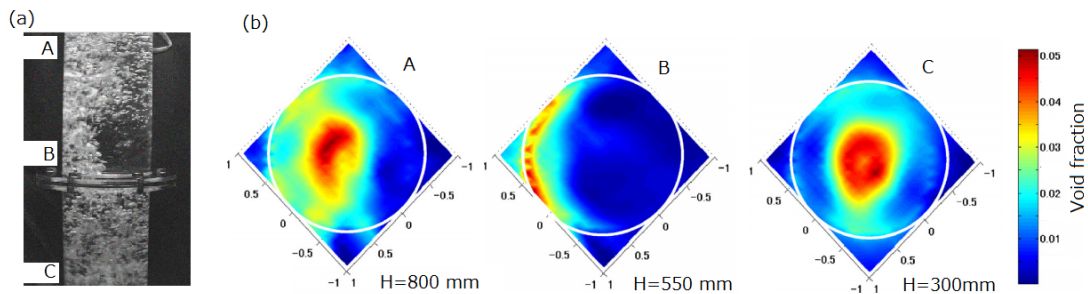


Fig. 20. Void fraction distribution in a bubble column with a baffle (Supardan et al., 2007): (a) snapshot of a 160-mm-diameter column and three measurement sections with six pairs of emitters and receivers attached in parallel; (b) corresponding mean void fraction distributions when section B has a baffle.

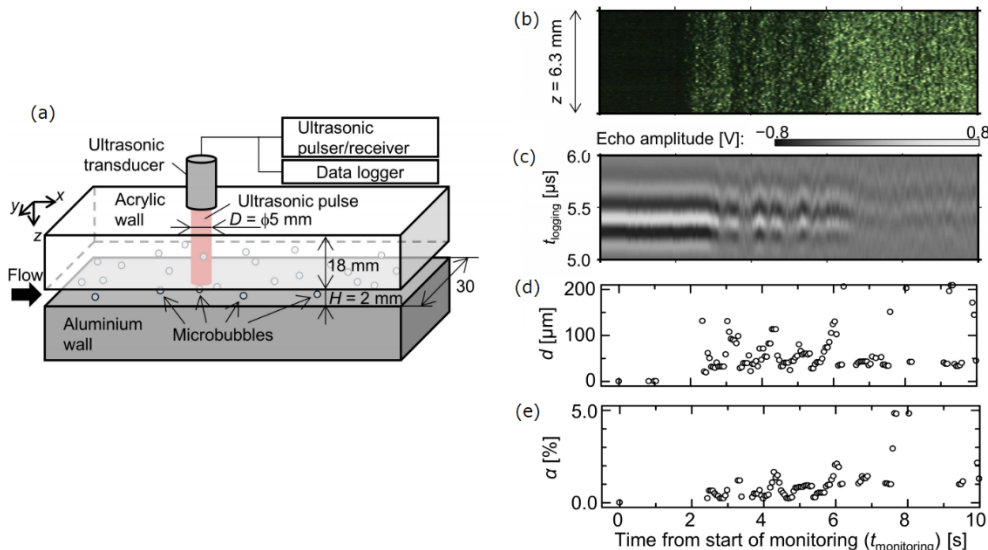


Fig. 21. Ultrasound pulse sensing of microbubbles passing by a channel (Park et al., 2021): (a) measurement set-up (the flow speed is 0.6 m/s); (b) optical line-scanned image of microbubbles; (c) pulse-echo waveform distorted by microbubbles; (d) measured instantaneous bubble diameter; (e) measured void fraction.

For dilute bubbly flows, individual positions of bubbles are directly detected via pulse-echo intensity profiles obtained along multiple transducers from different angles (Masala et al., 2007; Murakawa et al., 2008).

For example, [Nguyen et al. \(2016b\)](#) measured the vapor bubble distribution with two transducers in a vertical column, and determined the local volumes of sub-cooled bubbles along with the average condensation rate, as shown in **Fig. 22**.

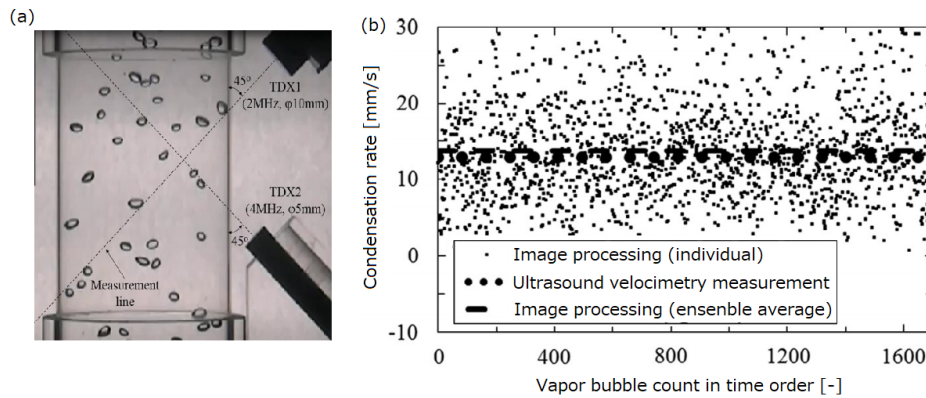


Fig. 22. Condensation rate of vapor bubbles determined by [Nguyen et al. \(2016b\)](#) from the velocity difference between two ultrasonic measurement lines: (a) sub-cooled bubble images in a 52-mm-diameter column; (b) condensation rate as an ensemble-averaged value.

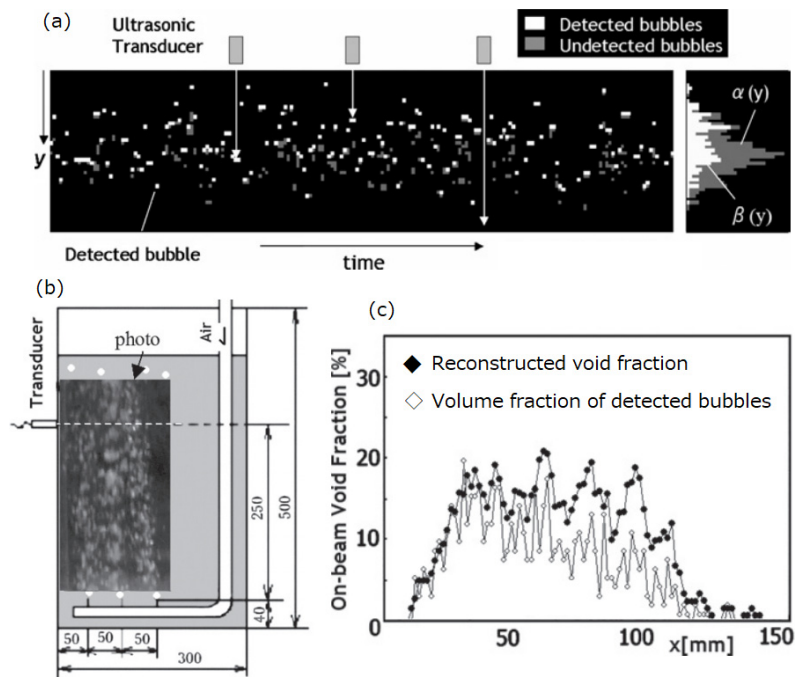


Fig. 23. Ultrasound pulse profiling of the void fraction in bubbly flow ([Murai et al., 2009](#)): (a) relationship between detected and undetected bubbles; (b) aeration chamber measurement; (c) resultant void fraction profile.

In general, the pulse-echo intensity method allows for accurate detection of only the gas bubble nearest to the transducer, and the accuracy decreases with increasing depth in bubbly liquids. A tracking technique has been developed for measuring multiple bubbles concurrently with good accuracy at an average void fraction of around 1% ([Povolny et al., 2018](#)). The key point is to distinguish between different bubbles using the reflection strength/amplitude combined with the measurement time (number of pulse emissions) and

position (time of flight). An alternative method is to use the following statistical relationship between the nearest bubbles and the real distribution:

$$\alpha(y) = \beta(y) \left(1 - \frac{1}{\delta} \int_0^y \beta(y) dy \right)^{-1}, \quad (17)$$

where α is the real void fraction profile and β the nearest bubble fraction profile, corresponding to **Fig. 23(a)**. [Murai et al. \(2009\)](#) examined the feasibility of this approach for various bubbly flows including aeration [**Fig. 23(b,c)**], upward bubbly jets, and bubbles in wall-turbulent shear flows.

3.3.2 Distinguishing bubbles and particles

To simultaneously measure the velocity of gas bubbles and liquid flow, the liquid should be seeded with small particles. As a result, the data measured via PWUD contain the velocity information of both phases. Although the particle velocity can be regarded as the liquid velocity by ignoring the slippage between the liquid and seeding particles, separating the liquid and gas velocities from the measured signal is still a challenge. Because the velocity of bubbles is usually different from that of the liquid phase, especially in a vertical pipe, a statistically based phase-separation method was proposed to detect the bubble positions and hence separate the velocities of the bubbles and liquid phase from the mixture velocity profile ([Aritomi et al., 1996](#); [Zhou et al., 1998](#)). It is based on the PDF of all measured velocities at each measuring position, of which two peaks represent the velocities of the liquid and the rising bubble respectively. Examples are the liquid flow structure around a bubble and turbulence intensity in vertical bubbly flow at a void fraction lower than 3% ([Murakawa et al., 2003](#)). [Suzuki et al. \(2002\)](#) proposed another phase-separation method using the pattern recognition of each instant velocity profile (i.e., the local maximum velocity) to identify the bubble interface. This method was verified in counter-current vertical bubbly flow with a void fraction lower than 7%.

The above two-phase separation methods are based on the interphase velocity difference and can only be applied in limited flow conditions. The separation becomes poor when the velocities of both phases are similar ([Nguyen et al., 2016a](#)). Additionally, the echo intensity reflected from a bubble is stronger than from a particle owing to the differences in acoustic impedance and diameter, which also can be used to separate different phases. The ultrasound echo signal is sensitive to the size of the scatterers relative to the sample volume/beam diameter. For example, in vertical upward bubbly flow where the rising velocities of the liquid and bubble differ greatly, an increase in transducer diameter D_{us} causes a decrease in ultrasonic reflection on the particle as compared with the bubble. As a result, most of the recorded velocities in the velocity PDF significantly vary with D_{us} , as shown in **Fig. 24**. The velocity PDF peaks at a mean low particle (liquid) velocity when the beam diameter is small ($D_{us}=2.5$ mm), and moves to the mean bubble rising velocity as D_{us} increases to 10 mm. Therefore, the velocities of several types of scatterers whose sizes differ greatly can be separated by choosing a proper transducer diameter.

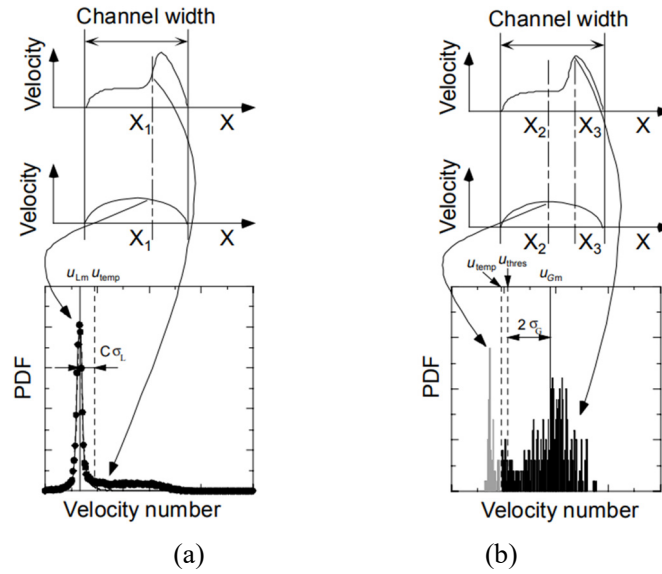


Fig. 24. Separation of the velocity distributions of the gas and liquid phases using statistical methods: (a) PDF obtained using all velocities at each measuring point; (b) PDF obtained using the maximum velocity in the channel (Murakawa et al., 2003).

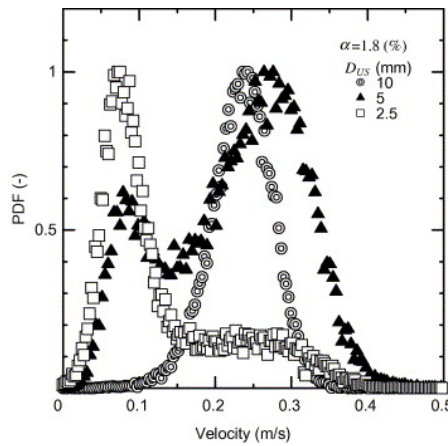


Fig. 25. Example of a velocity PDF at a measurement position for different transducer beam diameters (Murakawa et al., 2005).

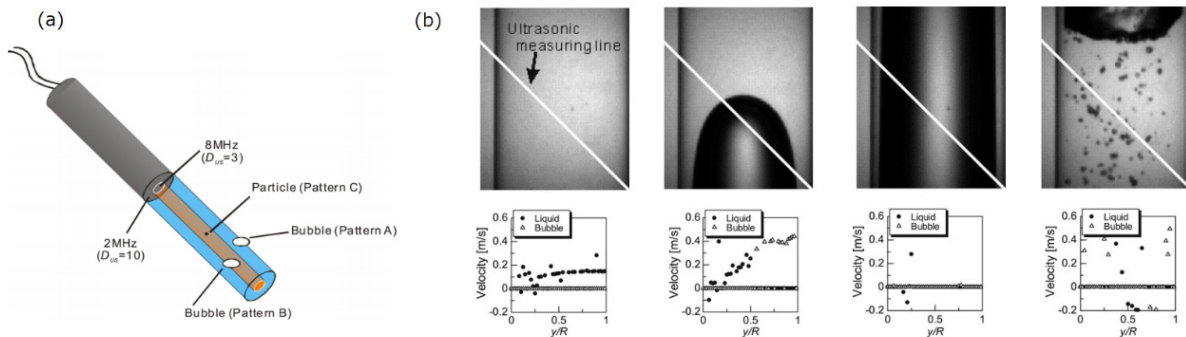


Fig. 26. Separation of particle and bubble echo signals proposed by Murakawa et al. (2008): (a) coaxial multi-wave transducer for signal separation; (b) bubble and tracer particle velocity plots (plots at zero mean no data within the given space-time spots).

Using this idea and the PDF statistical method, [Murakawa et al. \(2005\)](#) designed a multi-wave coaxial transducer that comprises two separate concentric cylindrical piezoelectric elements with different diameters and frequencies to measure the velocity profile of each phase, as shown in **Fig. 26(a)**. Because the bubbles are much larger than the particles, the outer element with a 10-mm diameter and 2-MHz frequency mainly measures bubble velocity, and the central element with a 3-mm diameter and 8-MHz frequency mainly measures particle (liquid) velocity in co-current vertical gas–liquid flow. However, the liquid flow velocity is also sensed by the 2-MHz element, which may result in errors in estimating the bubble rising velocity. Therefore, a threshold based on the relative velocity is needed in velocity PDFs to separate the liquid and gas velocities. This is implemented with a cross-correlation signal processing technique (ultrasound time-domain correlation, UTDC) ([Murakawa et al., 2008](#)). On the basis of the intensity differences of the echo signals reflected from the particles and gas–liquid interfaces, the combination of the echo signals at 2 MHz and 8 MHz has three patterns according to the presence of the particles and bubbles. The signal comparison led to development of a new phase-separation method based on pattern recognition of thresholding echo signals at 2 MHz and 8 MHz to distinguish the echoes from bubbles and particles. This method synchronizes the measurement of liquid and gas velocity profiles at the same position at a sampling rate of 1000 Hz in bubbly flow [**Fig. 26(b)**]. Compared with the previous UDM ([Murakawa et al., 2005](#)), UTDC measures the velocity of both phases without needing the relative velocity at a high time resolution, and it improves the accuracy of bubble velocity profiling owing to the strong echo reflected by bubbles ([Kikura et al., 2009](#)). However, the error in the liquid velocity increases with the bubble rising velocity, especially at low SNR, so the success rate of calculating the velocity with the UTDC method is relatively low owing to its high sensitivity to noise.

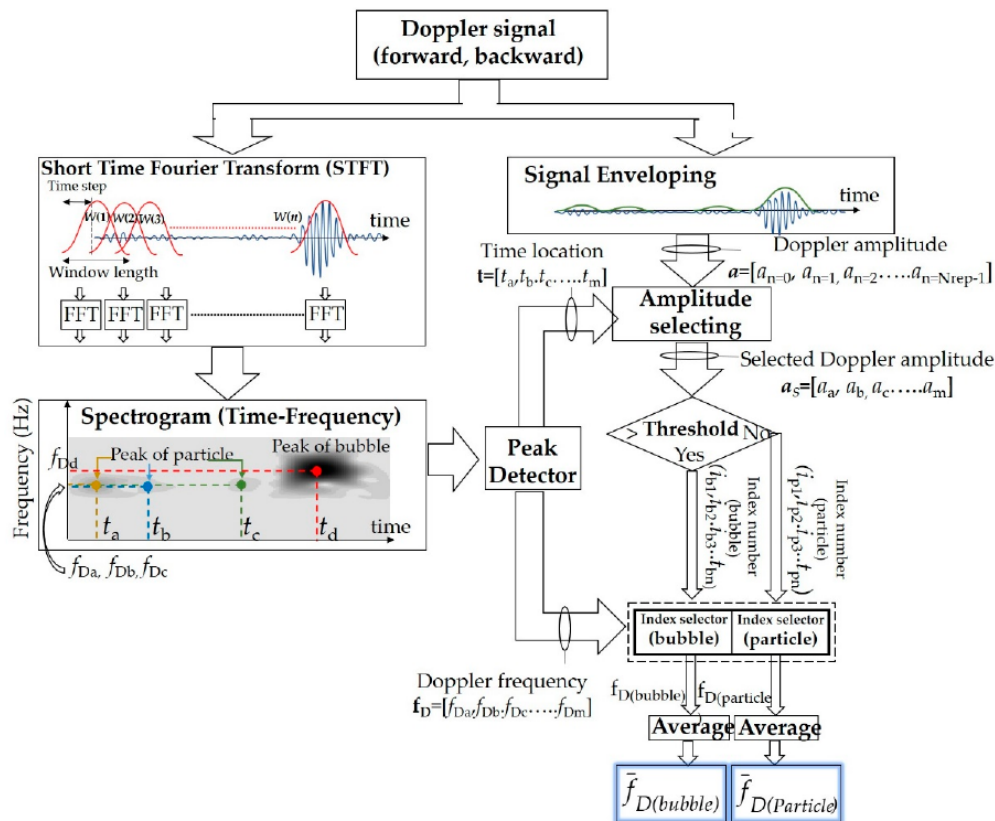


Fig. 27. Block diagram of the phase-separation technique to separate liquid and bubble velocities in one measurement channel ([Wongsaroj et al., 2019](#)).

To further improve the robustness to noise, [Nguyen et al. \(2016a\)](#) developed a new multi-wave UDM-based PWUD method with spike excitation and autocorrelation echo processing. With autocorrelation ([Nguyen et al., 2013a](#)), the velocity is calculated at low SNR, and the short spike excitation signal improves the spatial resolution (in a small sample volume). The average bubble velocity profile has been measured with PIV in counter-current vertical bubbly flow with a void fraction less than 10%, showing the applicability and robustness of this method.

Although a multi-wave transducer is preferable for measuring the instantaneous velocity profile of both liquid and bubbles, the number of pulser-receivers and data processing units need to be doubled to process two frequencies. Therefore, to reduce the system complexity and cost, a single-frequency technique is desired to simultaneously obtain the velocity profiles of both phases. Because the ultrasonic Doppler echoes from the bubble and particle are different in amplitude and frequency owing to their differences in size, acoustic impedance, and velocity, the two phase velocities can be separated using an FFT with a fixed window incorporated with Doppler amplitude classification ([Wongsaroj et al., 2017](#)). However, the measurement accuracy deteriorates when the Doppler signals produced by the particle and bubble both occur in the same window. To mitigate this effect, [Wongsaroj et al. \(2019\)](#) developed Doppler frequency decomposition based on time-frequency analysis (short-time Fourier transform, STFT) and Doppler amplitude classification, as shown in **Fig. 27**, delivering a measurement error within $\pm 10\%$ for both phase velocity profiles. This technique was then extended to measure the 2D velocity vector profiles of both phases in bubbly flow using one transmitter and two receivers ([Wongsaroj et al., 2020](#)).

3.4 Slug and film flow velocity measurement

Gas–liquid two-phase slug flow is a typical intermittent flow pattern composed of a liquid slug entrained with small bubbles, a liquid film, and a gas pocket. According to the relationship between echo intensity and particle size, [Yin et al. \(2020\)](#) used an 8-MHz transducer with a diameter of 3 mm and a 2-MHz transducer with a diameter of 5 mm to respectively measure the liquid velocity profiles in the liquid film zone and liquid slug zone. The velocity profile of the liquid slug, in which seeding particles and gas bubbles co-existed, was distinguished from the bubble velocity using the echo intensity. The boundary layer in a liquid film can also be extracted from the velocity profiles by placing a transducer parallel to the flow direction at the pipe bottom ([Wang et al., 2020](#)). On the basis of the liquid velocity measured in the liquid film/slug zone, a quantitative method was developed to distinguish and classify the separated flow, slug flow, and plug flow.

CWUD is capable of estimating the average velocity of the dispersed phase in a sample volume ([Dong et al., 2017](#)). However, CWUD with sensors on opposite sides may fail to receive ultrasound echoes when large gas bubbles block the transmission path (**Fig. 7**). Therefore, CWUD with sensors on the same side, in which the sample volume occupies the whole pipe cross section (**Fig. 3**), can be used to measure gas–liquid two-phase flow under different flow regimes. In this configuration, the measured average Doppler velocity (average velocity of the gas phase) does not equal the gas superficial velocity or overall superficial velocity owing to the interphase slippage. Therefore, a two-fluid model and slug closure model were introduced whereby fluid force analysis is used to correlate the superficial velocity of the individual phase and the overall superficial velocity under different flow regimes in horizontal gas–liquid two-phase flow ([Dong et al., 2017](#)). The average Doppler shift $\langle f_d \rangle$ measured via CWUD directly relates to the gas velocity in bubble flow and plug flow as well as the bubble velocity in the slug body region. This has led to measurement models based on two-fluid and slug-closure models that correlate $\langle f_d \rangle$ with the individual or overall flow velocity, which is compensated by the water holdup measured with a conductance sensor ([Shi et al., 2021](#)). The

measurement error (defined as the ratio of the difference between the reference and the measurement to the reference) of the superficial flow velocity is within 5%.

Owing to the intense fluctuations in phase fraction and velocity in slug flow, the bubbles in different regions of the slug body produce different $\langle f_d \rangle$ values. As a result, a Doppler signal with multi-scale fluctuations contains the structural velocities of slug flow, which can be decomposed through joint time-frequency analysis with the Doppler signal and holdup signal (Shi et al., 2019; Shi et al., 2021). Empirical mode decomposition was used to decompose the Doppler signal into intrinsic mode functions, which were combined with the water holdup to classify different flow structures (i.e., identify the specific phase) and determine the velocities of the liquid slug nose, liquid slug body, and film.

3.5 Particulate two-phase flow

For particulate two-phase flow, profiling of liquid velocity via PWUD and particle concentration via pulse-echo intensity can be conducted simultaneously to visualize the flow structure. Fig. 28 presents the two-line measurement of a turbidity current in a laboratory flume conducted by Hitomi et al. (2020). The particle concentration was estimated from acoustic attenuation theory for suspension flow (Lee and Hanes, 1995). The Reynolds shear stress due to vertical density stratification was found to be canceled, which explained the reduced kinetic energy dissipation during horizontal migration of the current.

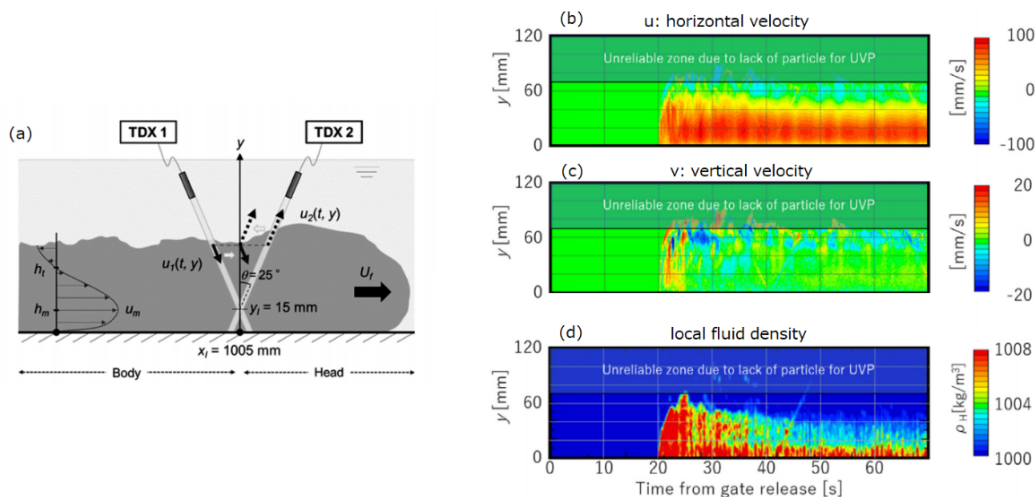


Fig. 28. Two velocity components of a turbidity current measured by Hitomi et al. (2020): (a) arrangement of transducers; (b) horizontal velocity evolution; (c) vertical velocity evolution; (d) local fluid density distribution.

Additionally, the two-dimensional velocity of large particles can be measured through ultrasonic imaging velocimetry (UIV) when the flow speed is slow. Fig. 29 shows velocity profiles of particles stratified owing to gravity (Gurung and Poelma, 2016). Because UIV directly visualizes particle images using echography in two dimensions, the volume fraction and flow speed of the particles are obtained simultaneously.

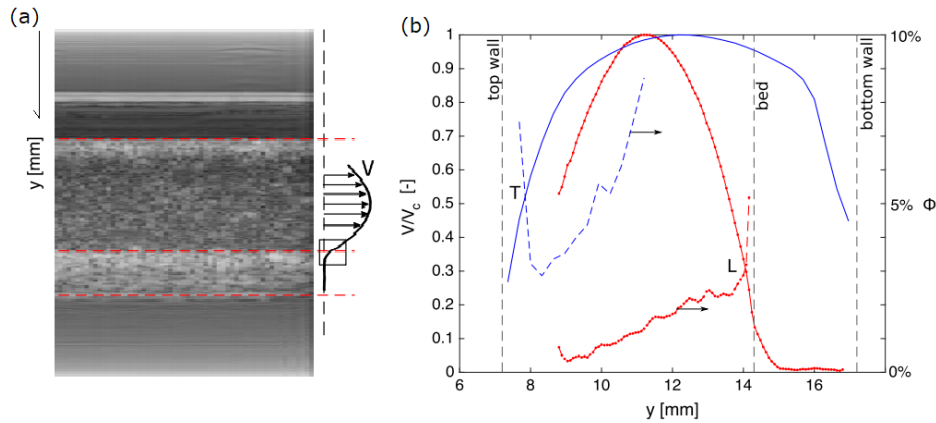


Fig. 29. Ultrasound imaging velocimetry used by [Gurung and Poelma \(2016\)](#) to measure particulate flow: (a) scanned echo image of particles flowing in a pipe with an immobile particle layer; (b) mean streamwise particle velocity profile for the laminar (L) and turbulent (T) cases, where dashed lines represent the local particle concentration on the secondary axis.

3.6 Three-phase flow measurement

There is growing demand for measuring three-phase flows such as for slurry air-lift pumps (gas–liquid–solid) and petroleum pipelines (gas–liquid–liquid). Most of these fluids are opaque, so ultrasound monitoring is strongly needed. In various combinations of three phases, oil–gas–water three-phase flow exhibits the most variable interfacial behaviors because two kinds of deformable fluid–fluid interfaces govern the flow. In oil–gas–water three-phase flow, the dispersed liquid (oil or water) droplets and gas bubbles are the natural scatterers of ultrasound, so the reflected ultrasonic Doppler signal is a complicated multi-frequency combination that contains different phase velocities. However, when the gas volume fraction α_G varies from 0 to 75%, the average flow velocity calculated by integrating the velocity profile correlates neither with the reference liquid velocity nor the homogeneous velocity, and the flow velocity is underestimated when α_G is increased ([Huang et al., 2013](#)). One reason is the reduced ultrasonic interrogation depth into the mixture due to the increased bubbles in the liquid. As a result, it is difficult to interpret the Doppler velocity and derive the flowrates of three-phase flow without an elaborate flow model. Because the $\langle f_d \rangle$ value measured through CWUD is related to the average physical velocity of two dispersed phases in three-phase flow, the two-fluid model can be modified for three-phase flow by analyzing the momentum balance between different phases. A new theoretical model was derived to estimate the superficial velocity of an individual phase with a measurement error within 5% ([Tan et al., 2018](#)).

In gas–oil–water three-layer stratified flow, the instantaneous velocity profile obtained via PWUD was found to be affected by refraction at the oil–water interface, and the bias in velocity magnitude was attributed to the interface curvature ([Hitomi et al., 2017](#)). A simple three-phase vertical stratification model was used to obtain the flowrate of each phase by spatially integrating the velocity profile within each phase area. The interface of each phase was identified from the echo intensity profile with a measurement error less than 10%. **Fig. 30** shows the results of both the interface and Doppler velocity measurements for air–oil–water three-phase slug flow in a horizontal pipe. However, in other flow patterns, the complex structure and distribution of the three phases make it more difficult to separate the information than in gas–liquid two-phase flow. The concentration of the liquid droplets in three-phase flow is much higher than that of the seeding particles in two-phase flow, leading to different flow statuses in the liquid–liquid mixture, so the reflected signals from the liquid and gas are superposed and contain rich flow velocity information for

different phases in different frequency bands. More sophisticated signal processing algorithms are needed to separate the flow velocities of the liquid and gas, and another sensor is usually required to support decomposition of the three velocities. For instance, a joint time-frequency analysis of empirical mode decomposition was applied to three-phase water-based dispersed flow to directly extract the velocity of individual phases by combining CWUD with a conductance sensor (Shi et al., 2019).

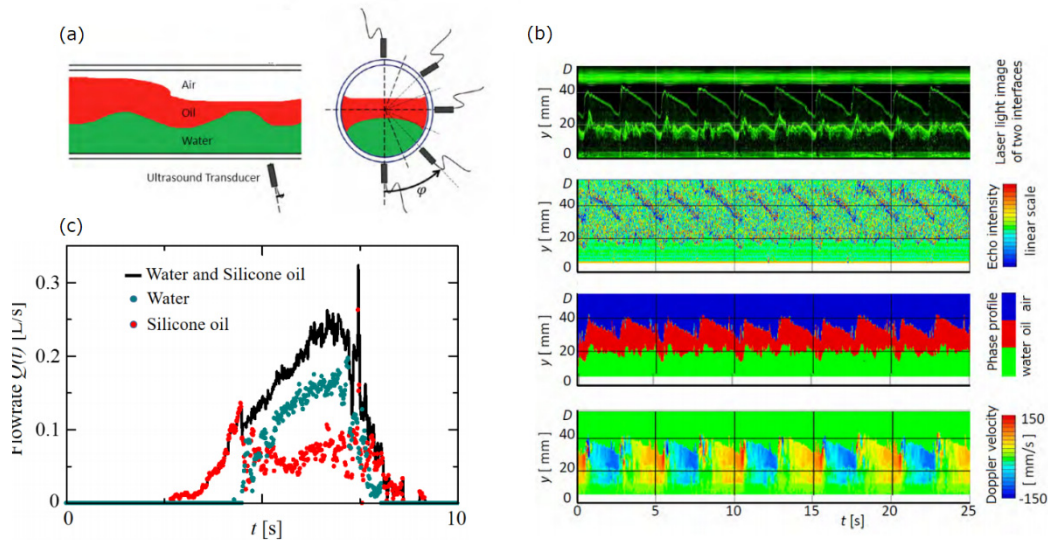


Fig. 30. Interface and flow rate of stratified air–oil–water three-phase slug flow in a horizontal pipe measured by Hitomi et al. (2017): (a) measurement set-up; (b) sensing of air–oil and oil–water interfaces and corresponding velocity profiles; (c) instantaneous component volume flow rates within a single slug passage.

3.7 Flow regime identification

Flow regime identification is fundamental to monitoring multiphase pipe flow, and is typically achieved using information such as the interfacial structure, velocity profile, and pressure fluctuation. Ultrasound can detect fluid interfaces and velocity to identify a flow regime non-intrusively. Examples are echo-intensity-based flow regime identification for a vertical two-phase pipe flow, where echo intensity clearly correlates with instantaneous void fraction (Figueiredo et al., 2016).

Because an ultrasonic Doppler signal also contains rich information on phase fluctuation and velocity, the frequency-domain features of a Doppler signal such as power spectral density and discrete wavelet transform are sensitive to change in flow structure. These features are fed into a multilayer perceptron neural network to recognize the regimes of slug flow, stratified flow, elongated bubble flow, and stratified wavy flow at a success rate up to 95.8% (Abbagoni and Yeung, 2016). To identify more flow regimes, principal component analysis was used to reduce the dimensionality of frequency-domain power spectral density features and identify bubbly, slug, churn, and annular flows at a success rate of 84.6% using a support vector machine (Nnabuife et al., 2019). The difficulty of separating annular and stratified flows is attributed to their similar features in the frequency domain. This is because the ultrasonic Doppler signal is not induced by the real flow velocity, but by the gas–liquid interfacial wave propagation velocity in these two regimes, which leads to erroneous identification. To improve robustness, a convolutional neural network was applied by Zhang et al. (2020) to a horizontal two-phase flow. Such study with machine learning is now rapidly increasing.

Flow regimes can also be classified using features of the frequency spectrum of an ultrasonic Doppler

signal in oil–water two-phase flow. These features include spectral broadening, distribution shape, amplitude, and power. This is because the governing factors of flow regimes, including the flow velocity and its distribution as well as the number and distribution of dispersed phases, jointly affect the Doppler signal. Experimental research has found that the spectral bandwidth is broadened by the velocity profile and number of droplets within a sample volume. The amplitude of each frequency shift component in the Doppler spectrum is proportional to the droplet number and concentration, and the spectral shape varies with flow regime. These correlations can be used to identify flow regimes with a success rate above 94% (Liu et al., 2021b), as shown in Fig. 31.

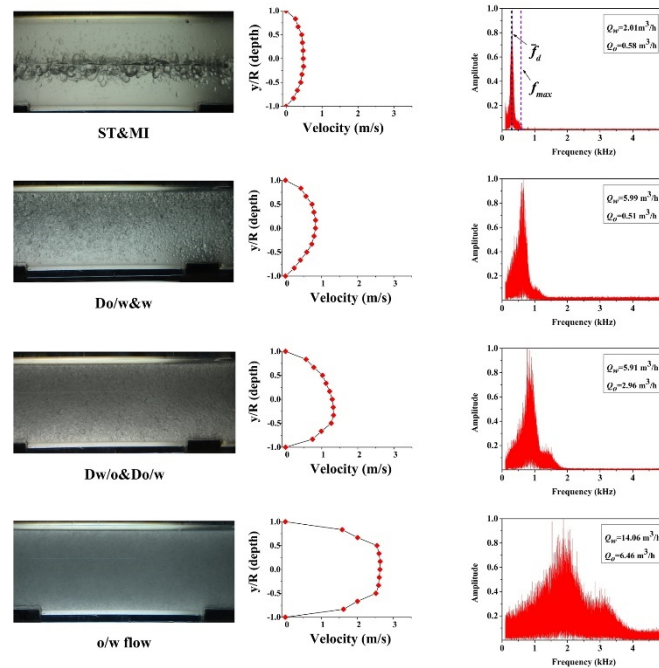


Fig. 31. Typical oil–water two-phase flow patterns with their corresponding ultrasonic Doppler spectrums, reproduced from (Liu et al., 2021b).

The intermittent flow structures in plug and slug flows cause corrosion and intense fluctuations in pressure and momentum, which have a significant impact on pipeline safety (Yin et al., 2018). Compared with bubbly flow, intermittent flow patterns have more complex hydrodynamics and structure due to the drastic phase interactions. Both PWUD and CWUD can distinguish gas–liquid two-phase flow patterns (Wang et al., 2020) and characterize the formation and development of intermittent flow. This is achieved by measuring the gas–liquid interface and liquid film thickness as well as the frequency, length, and velocity of the slug body (Shi et al., 2018; Yin et al., 2020), showing high potential for diagnosing multiphase flow processes.

3.8 2D velocity profiling of multiphase flow

Swirling flow is well recognized for enhancing heat transfer, assisting pneumatic conveying, and separating gas or solid particles from liquid. Conventional PWUD can obtain gas/liquid phase information and characterize swirling flow through the liquid film and 1D velocity profile (Liang et al., 2016), and evaluate heat transfer performance of bubbly swirling flow through the bubble velocity profile and void fraction (Hamdani et al., 2016b). To further characterize the 2D velocity field of the swirling flow, more projections of incident ultrasound should be used to collect velocity components in different directions. This could be

implemented with a phased-array transducer and cross-beam technique with beam forming, as shown in **Fig. 32** [错误!未找到引用源。](#) ([Hamdani et al., 2016a](#)). Dual-plane and two-component flow velocity measurements have been performed using four linear-transducer arrays, with each array comprising 25 elements for mapping the flow velocity distribution over the measurement plane ([Büttner et al., 2013](#)). The four transducer pairs can be arranged in arbitrary configurations and operated in parallel to transmit the ultrasonic pulses via different elements to calculate the Doppler velocity. The complex and transient local structure of the primary flow can be investigated using the two-component velocity distribution measured through a dual-plane configuration of the transducer array. Both the primary and secondary flows are mapped simultaneously through a crossed-plane configuration. Compared with conventional PWUD, the array transducer can map the multi-dimensional flow velocity field with high spatial accuracy to study the flow fields and their temporal evolution such as non-stationary or turbulent behavior. This has considerably advanced fluid dynamics research and industrial applications ([Batsaikhan et al., 2017](#); [Franke et al., 2013](#); [Mader et al., 2017](#); [Munkhbat et al., 2018](#)).

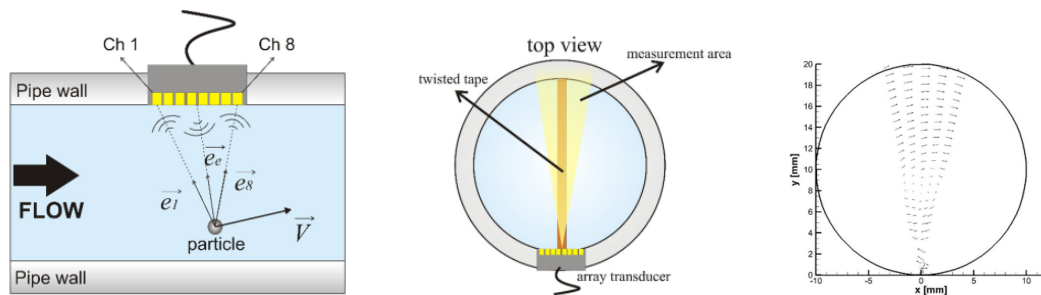


Fig. 32. 2D velocity field measurement with a phased-array transducer in swirling flow: (a) velocity vector reconstruction with a linear-array sensor; (b) set-up of a phased-array transducer for measuring tangential velocity; (c) 2D flow map of the velocity field in swirling flow ([Hamdani et al., 2016a](#)).

In an industrial plant, the pipeline usually comprises many long straight pipes with branches and bends, accompanied by abrupt contractions or enlargements ([Kotzé et al., 2011](#)). These affect the flow structure and production safety. In such applications, the 2D velocity field obtained via phased-array PWUD helps reveal the non-axisymmetric flow field in complex geometries, for instance, the 2D velocity distribution downstream of a 90° double bend under a swirling inlet ([Shwin et al., 2017](#)).

3.9 Measurement of multiphase flow rheology

Rheological properties are important fluid dynamics parameters that describe multiphase flow such as emulsion and suspension flows. The relationship between these rheological properties and resultant velocity distributions has been of great interest in non-Newtonian fluid mechanics. In CFD simulations, rheological properties are required before the flow field is computed. A conventional torque-spinning rheometer using a narrow gap cannot evaluate the properties of multiphase fluids correctly in most cases, because of the finite interfacial length scales compared with the narrow gap as well as the inhomogeneous distribution in the test fluids. PWUD can be used to estimate the rheological properties from the measured velocity distribution, which is an alternative and effective method for on-line measurement of temporal/spatial rheological evolution of multiphase flow ([Haavisto et al., 2017](#); [Kotzé et al., 2015](#)). For pipe flows, the bulk-averaged value of a rheological property is obtained by determining the wall shear stress and unsteady pipe friction from the transient velocity profile ([Brunone and Berni, 2010](#); [Brunone et al., 2000](#)). Research using PWUD includes pipe

flow rheometry, spinning rheometry, and viscosity distribution measurement coupled with momentum equations.

Ultrasound pipe flow rheometry determines the rheological properties of fluid through the velocity profile (using UVP) and pressure drop (PD), that is, the UVP-PD technique (Choi et al., 2006; Ouriev and Windhab, 2002; Wunderlich and Brunn, 1999). Pipe flow UVP-PD rheometry assumes an incompressible fluid with a steady pressure gradient in the laminar regime. The relationships between the shear stress σ , pipe radius r , shear rate $\dot{\gamma}(r)$, and apparent viscosity η of the pipe flow are

$$\sigma(r) = \frac{\Delta P \cdot r}{2L}, \quad \dot{\gamma}(r) = \frac{du(r)}{dr}, \quad \eta(r) = \frac{\sigma(r)}{\dot{\gamma}(r)}, \quad (18)$$

where ΔP is the pressure drop over the pipe length L , u is the axial flow velocity, and $u(r)$ is the velocity profile along the pipe radius. The relationship between the shear rate and shear stress of the fluid, which is called the fluid characteristic curve or “flow curve”, can be plotted to describe the rheological parameters through non-linear fitting using a suitable rheological model or via the velocity profile and pressure drop. UVP-PD rheometry has been successfully used for on-line rheological characterization of particle suspension pipe flows such as sludge flow (Ricci et al., 2017), and in fluids with dispersed phases such as fibers, emulsions, or colloidal polymers. Kotzé et al. (2016) summarized recent studies on UVP-PD rheometry for on-line rheological characterization and flow visualization from the aspects of methodology, optimization, and measurement procedures.

Measuring rheological properties with a spinning rheometer involves the “Couette inverse problem”, that is, the expected velocity profile in the cylinder differs from the actual velocity profile when one tries to derive the flow curve from measurements of torque and angular velocity in a coaxial double-cylinder rheometer. Ancy (2005) solved the inverse problem with wavelet-vaguelette decomposition to recover the shear rate, which is accurate and converges fast. Heirman et al. (2008) used integration to convert the torque to a flow curve for a wide-gap concentric-cylinder rheometer, and the flow resistance and power-law flow behavior were decoupled. The rotating cylinder generates a quasi-one-directional shear flow, and PWUD measures the velocity profile. Hence, the local rheological properties can be obtained over the shear rate.

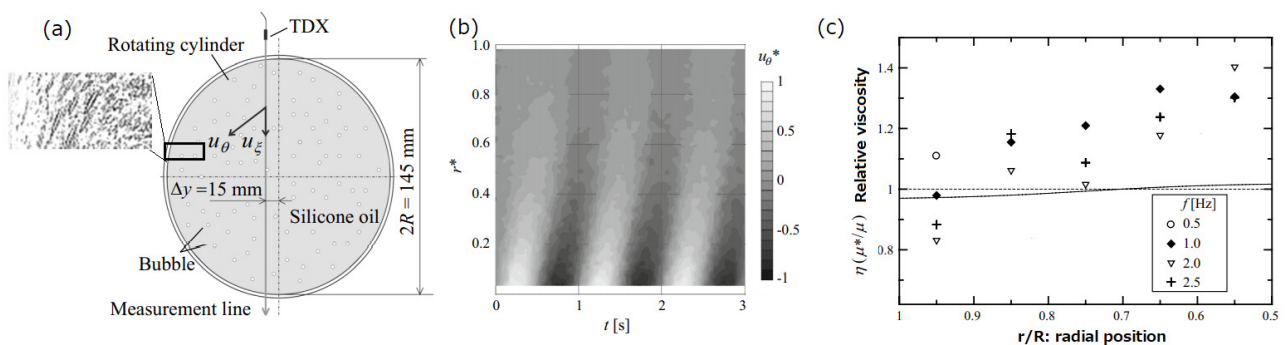


Fig. 33. Effective viscosity of bubbly liquid measured by Tasaka et al. (2014) with ultrasound spinning rheometry: (a) spinning container; (b) cyclic oscillation of azimuthal velocity measured with UVP; (c) viscosity profile influenced by the oscillation frequency.

The spatial-temporal information on the shear rate can be derived from the velocity profile measured via PWUD, which has been used for steady flow (Shiratori et al., 2015) and oscillatory shear flow (Tasaka et al., 2014). As a result, ultrasound spinning rheometry (USR), which combines PWUD and a rotating cylinder, is a

new spinning type of rheometry for estimating the effective viscosity. **Fig. 33** presents its application in bubbly liquids, where the effective viscosity is significantly higher than in steady shear flow owing to unsteady deformation of bubbles. The group at Hokkaido University extended this technique to various types of non-Newtonian multiphase fluids including solid particles, clay suspensions, and more complex multiphase media. This group established a new algorithm for more robust evaluation of local effective viscosity against measurement noise using the phase-lag information of oscillating shear propagation, and applied it to bubble suspensions (Tasaka et al., 2014). A frequency-domain algorithm was presented to overcome the measurement noise in the rheological assessment for the linear viscoelasticity of bubble suspensions (Tasaka et al., 2018). Various rheological properties of thixotropic fluid, shear-thinning fluid, and multiphase fluid were investigated with the phase-lag information extracted from spatial-temporal velocity data (Yoshida et al., 2017). Rheological evaluation with USR and its efficacy for non-Newtonian fluids were studied and found to agree well with determination via a parallel-disk spinning rheometer for a carboxymethyl cellulose (CMC) solution (Yoshida et al., 2019). The rheology of bubbly liquids and foam are quite complex and sensitive to disturbance, so non-invasive PWUD measurement can be a powerful tool to produce a breakthrough in experimental rheology. However, foam strongly absorbs ultrasound, making it a challenge to keep the SNR of ultrasound measurement. Nauber et al. (2018) applied PWUD with five arrangements of a low-frequency transducer at 175 kHz, as shown in **Fig. 34**. An ultrasound echo was obtained from film-cross points distributed in the foam, and thus the Doppler shift profile was analyzable to determine the foam velocity field.

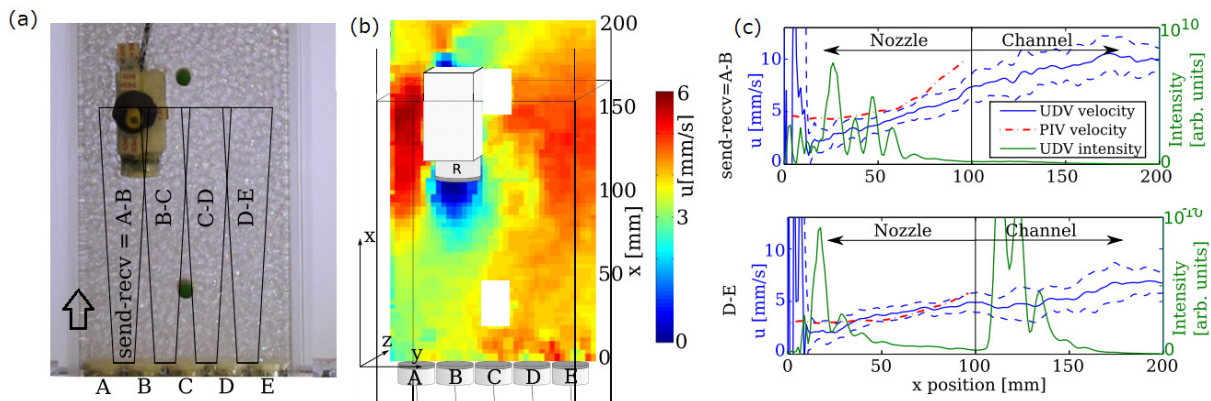


Fig. 34. Foam flow measurement by Nauber et al. (2018): (a) picture of the foam and the measurement volumes; (b) vertical velocity distribution measured via optical cross correlation; (c) ultrasound pulse measurement.

4. Summary and future prospects

The ultrasonic Doppler technique and its combination with echo intensity have gained increasing popularity in multiphase fluid dynamics research and industrial process monitoring and have been adapted quickly to meet more demands. Advantages that propel its application are its non-invasiveness in that it does not disturb fluid interfaces, and a high sampling rate with a small memory size allowing real-time or on-line measurement. Ultrasound is especially favorable for measuring opaque or non-transparent fluids, which shows great prospect for measuring multiphase flow. The future trends of ultrasonic measurement include:

1) From a 1D velocity field to a 2D velocity profile. Multiphase flow commonly shows asymmetrical structure and velocities, so there is an urgent need to use multi-line or array transducers to improve

three-dimensional monitoring or investigation of transient (local) structures of multiphase flows. This needs to go beyond the present framework for measuring velocity by introducing inter-correlation of multi-directional projections from an arrangement of multiple transducers such as an ultrasonic phased array, along with more sophisticated algorithms to be implemented in advanced and high-performance hardware. UIV (Poelma, 2016), which is now limited to slow flows, is one of the main candidates for extension. Additionally, the ultrasonic phased array has been widely applied in medical imaging, so it also has promising use in multiphase flow velocity profiling (Ricci et al., 2017) and phase distribution tomography (Liu et al., 2021a). By combining multiple modes of ultrasound propagation in multiphase flow, one could jointly reconstruct the phase and velocity distribution through ultrasonic phased-array probes.

2) From single-frequency to multi-frequency. Because the multiphase flow usually has dispersed phases with multiple sizes, single-frequency ultrasound undergoes aliasing in the frequency domain. This could be compensated using multi-frequency ultrasound, but more advanced spectral analysis and parameterization techniques are required to improve the sensing accuracy. Additionally, the ultrasonic spectrum could provide phase separation (Liu et al., 2021a) and particle/droplet sizing (Yu et al., 2021), which combined with Ultrasound Doppler will greatly expand applications to multiphase flow measurement.

3) From insert to clamp-on. Multiphase flow under high/low temperature, Newtonian and non-Newtonian liquid flow, and convective heat transfer are within the realm of future research in engineering. Therefore, to achieve a ‘clamp-on’ sensor, further technical advancements are required to deal with the thick steel pipe wall (up to 100 mm thick) and highly attenuated fluids in large pipes such as sludge or slurry flow in industry. While a basic clamp-on device has already been designed and used for single-phase pipeline systems, a future challenge is designing one that enables the more sophisticated signal processing needed for multiphase flow (Murakawa et al., 2020).

4) From physical modeling to data-driven and then hybrid modeling. Ultrasound Doppler echoes contain rich information regarding multiphase flow phase fraction and velocity distribution, which can be analyzed and synthesized with machine learning. This enables not only flow pattern identification but also quantitative monitoring of various complex multiphase flows that are difficult to model analytically. Consequently, real-time measurement via ultrasound opens a new area of data assimilation, that is, numerical coupling between measured and predicted information in real time, such as a digital twin. This will contribute to flow assurance and prediction, which has long been an unsolved issue in multiphase applications.

To conclude, the ultrasonic Doppler technique is a simple and low-cost measurement technique. Until now, most applications have been to low void fraction or homogeneous two-phase flow. More challenging measurements and characterizations of multiphase flow are needed to further explore the potential of the ultrasonic Doppler technique in scientific research and engineering design.

Acknowledgements

This work was supported by the National Key Research and Development Program of China (Grant No. 2019YFB1504702), National Natural Science Foundation of China (Nos. 61973229 and 51976137), Japanese Society for Promotion of Science (JSPS KAKENHI, No. 18KK0105), and New Energy Development Organization of Japan (NEDO, No. 19101191-0). The authors thank Prof. H. Murakawa of Kobe University and Prof. H. Kikura of Tokyo Institute of Technology for their cooperation.

Reference

Abbagoni, B.M., Yeung, H., 2016. Non-invasive classification of gas-liquid two-phase horizontal flow regimes

- using an ultrasonic Doppler sensor and a neural network. *Meas. Sci. Technol.* 27, 084002. doi: 10.1088/0957-0233/27/8/084002
- Al-Aufi, Y.A., Hewakandamby, B.N., Dimitrakis, G., Holmes, M., Hasan, A., Watson, N.J., 2019. Thin film thickness measurements in two phase annular flows using ultrasonic pulse echo techniques. *Flow. Meas. Instrum.* 66, 67-78. doi: 10.1016/j.flowmeasinst.2019.02.008
- Ancey, C., 2005. Solving the Couette inverse problem using a wavelet-vaguelette decomposition. *J. Rheol.* 49, 441-460. doi: 10.1122/1.1849181
- Ando, K., Colonius, T., Brennen, C.E., 2011. Numerical simulation of shock propagation in a polydisperse bubbly liquid. *Int. J. Multiphase Flow* 37, 596-608. doi: 10.1016/j.ijmultiphaseflow.2011.03.007
- Aritomi, M., Zhou, S., Nakajima, M., Takeda, Y., Mori, M., Yoshioka, Y., 1996. Measurement System of Bubbly Flow Using Ultrasonic Velocity Profile Monitor and Video Data Processing Unit. *J. Nucl. Sci. Technol.* 33, 915-923. doi: 10.1080/18811248.1996.9732033
- Baker, D.W., 1970. Pulsed ultrasonic Doppler blood-flow sensing. *IEEE Transactions on Sonics and Ultrasonics* SU-17, 170-185. doi:
- Baker, D.W., Yates, W.G., 1973. Technique for studying the sample volume of ultrasonic Doppler devices. *Medical and biological engineering* 11, 766-770. doi: 10.1007/BF02478666
- Batsaikhan, M., Hamdani, A., Kikura, H., 2017. Visualisation of air–water bubbly column flow using array Ultrasonic Velocity Profiler. *Theoretical and Applied Mechanics Letters* 7, 379-385. doi: 10.1016/j.taml.2017.09.014
- Brody, W.R., Meindl, J.D., 1974. Theoretical Analysis of the CW Doppler Ultrasonic Flowmeter. *IEEE Trans. Biomed. Eng.* BME-21, 183-192. doi: 10.1109/TBME.1974.324381
- Brunone, B., Berni, A., 2010. Wall Shear Stress in Transient Turbulent Pipe Flow by Local Velocity Measurement. *Journal of Hydraulic Engineering* 136, 716-726. doi: 10.1061/(asce)hy.1943-7900.0000234
- Brunone, B., Karney, B.W., Mecarelli, M., Ferrante, M., 2000. Velocity Profiles and Unsteady Pipe Friction in Transient Flow. *Journal of Water Resources Planning and Management* 126, 236-244. doi: 10.1061/(asce)0733-9496(2000)126:4(236)
- Büttner, L., Nauber, R., Burger, M., Rübiger, D., Franke, S., Eckert, S., Czarske, J., 2013. Dual-plane ultrasound flow measurements in liquid metals. *Meas. Sci. Technol.* 24, 055302 (055312pp). doi: 10.1088/0957-0233/24/5/055302
- Chakraborty, S., Das, P.K., 2020. Characterisation and classification of gas-liquid two-phase flow using conductivity probe and multiple optical sensors. *Int. J. Multiphase Flow* 124, 103193. doi: 10.1016/j.ijmultiphaseflow.2019.103193
- Chang, J.S., Morala, E.C., 1990. Determination of two-phase interfacial areas by an ultrasonic technique. *Nucl. Eng. Des.* 122, 143-156. doi: 10.1016/0029-5493(90)90203-a

Chemloul, N.S., Chaib, K., Mostefa, K., 2009. Simultaneous Measurements of the Solid Particles Velocity and Concentration Profiles in Two Phase Flow by Pulsed Ultrasonic Doppler Velocimetry. *Journal of the Brazilian Society of Mechanical Sciences and Engineering* 31, 333-343. doi: 10.1590/S1678-58782009000400008

Choi, Y.J., McCarthy, K.L., McCarthy, M.J., 2006. Tomographic Techniques for Measuring Fluid Flow Properties. *J. Food Sci.* 67, 2718-2724. doi: 10.1111/j.1365-2621.2002.tb08804.x

Claesson, J., Rasmuson, A., Wiklund, J., Wikström, T., 2013. Measurement and analysis of flow of concentrated fiber suspensions through a 2-D sudden expansion using UVP. *AIChE Journal* 59, 1012-1021. doi: 10.1002/aic.13881

Coutinho, F.R., Ofuchi, C.Y., de Arruda, L.V., Neves, F., Jr., Morales, R.E., 2014. A new method for ultrasound detection of interfacial position in gas-liquid two-phase flow. *Sensors (Basel)* 14, 9093-9116. doi: 10.3390/s140509093

de Azevedo, M.B., Faccini, J.L.H., Su, J., 2020. Experimental study of single Taylor bubbles rising in vertical and slightly deviated circular tubes. *Exp. Therm Fluid Sci.* 116, 110109. doi: 10.1016/j.expthermflusci.2020.110109

de Azevedo, M.B., Santos, D.d., Faccini, J.L.H., Su, J., 2017. Experimental study of the falling film of liquid around a Taylor bubble. *Int. J. Multiphase Flow* 88, 133-141. doi: 10.1016/j.ijmultiphaseflow.2016.09.021

Dong, F., Gao, H., Liu, W.L., Tan, C., 2019. Horizontal oil-water two-phase dispersed flow velocity profile study by ultrasonic doppler method. *Exp. Therm Fluid Sci.* 102, 357-367. doi: 10.1016/j.expthermflusci.2018.12.017

Dong, X., Tan, C., Yuan, Y., Dong, F., 2016a. Measuring Oil–Water Two-Phase Flow Velocity With Continuous-Wave Ultrasound Doppler Sensor and Drift-Flux Model. *IEEE Trans. Instrum. Meas.* 65, 1098-1107. doi: 10.1109/tim.2015.2507740

Dong, X.X., Tan, C., Dong, F., 2017. Gas-Liquid Two-Phase Flow Velocity Measurement With Continuous Wave Ultrasonic Doppler and Conductance Sensor. *IEEE Trans. Instrum. Meas.* 66, 3064-3076. doi: 10.1109/tim.2017.2717218

Dong, X.X., Tan, C., Yuan, Y., Dong, F., 2015. Oil-water two-phase flow velocity measurement with continuous wave ultrasound Doppler. *Chem. Eng. Sci.* 135, 155-165. doi: 10.1016/j.ces.2015.05.011

Dong, X.X., Tan, C., Yuan, Y., Dong, F., 2016b. Measuring Oil-Water Two-Phase Flow Velocity With Continuous-Wave Ultrasound Doppler Sensor and Drift-Flux Model. *IEEE Trans. Instrum. Meas.* 65, 1098-1107. doi: 10.1109/tim.2015.2507740

Duffey, R.B., Hall, R.S., 1969. An ultrasonic technique for measuring the transient movements of a liquid-vapour interface. *Journal of Physics E: Scientific Instruments* 2, 193-194. doi: 10.1088/0022-3735/2/2/318

Evans, D.H., McDicken, W.N., 2000. *Doppler Ultrasound: Physics, Instrumentation and Signal Processing*. John Wiley & Sons, LTD, Chichester, England.

- Figueiredo, M.M.F., Goncalves, J.L., Nakashima, A.M.V., Fileti, A.M.F., Carvalho, R.D.M., 2016. The use of an ultrasonic technique and neural networks for identification of the flow pattern and measurement of the gas volume fraction in multiphase flows. *Exp. Therm Fluid Sci.* 70, 29-50. doi: 10.1016/j.expthermflusci.2015.08.010
- Franca, M.J., Lemmin, U., 2006. Eliminating velocity aliasing in acoustic Doppler velocity profiler data. *Meas. Sci. Technol.* 17, 313-322. doi: 10.1088/0957-0233/17/2/012
- Franke, S., Lieske, H., Fischer, A., Buttner, L., Czarske, J., Rabiger, D., Eckert, S., 2013. Two-dimensional ultrasound Doppler velocimeter for flow mapping of unsteady liquid metal flows. *Ultrasonics* 53, 691-700. doi: 10.1016/j.ultras.2012.10.009
- Franklin, D.L., Schlegel, W., Rushmer, R.F., 1961. Blood flow measured by Doppler frequency shift of back-scattered ultrasound. *Science* 134, 564-565. doi:
- García, C.M., Cantero, M.I., Niño, Y., García, M.H., 2005. Turbulence Measurements with Acoustic Doppler Velocimeters. *Journal of Hydraulic Engineering* 131, 1062-1073. doi: doi:10.1061/(ASCE)0733-9429(2005)131:12(1062)
- Gonzalez A, S.R., Murai, Y., Takeda, Y., 2009. Chapter 1 Ultrasound-Based Gas–Liquid Interface Detection in Gas–Liquid Two-Phase Flows, *Characterization of Flow, Particles and Interfaces*, pp. 1-27.
- Gurung, A., Poelma, C., 2016. Measurement of turbulence statistics in single-phase and two-phase flows using ultrasound imaging velocimetry. *Exp. Fluids* 57. doi: 10.1007/s00348-016-2266-x
- Haavisto, S., Cardona, M.J., Salmela, J., Powell, R.L., McCarthy, M.J., Kataja, M., Koponen, A.I., 2017. Experimental investigation of the flow dynamics and rheology of complex fluids in pipe flow by hybrid multi-scale velocimetry. *Exp. Fluids* 58, 158. doi: 10.1007/s00348-017-2440-9
- Hamdani, A., Ihara, T., Kikura, H., 2016a. Experimental and numerical visualizations of swirling flow in a vertical pipe. *Journal of Visualization* 19, 369-382. doi: 10.1007/s12650-015-0340-8
- Hamdani, A., Ihara, T., Tsuzuki, N., Kikura, H., 2016b. Experimental study of bubbly swirling flow in a vertical tube using ultrasonic velocity profiler (UVP) and wire mesh sensor (WMS). *Journal of Mechanical Science and Technology* 30, 3897-3905. doi: 10.1007/s12206-016-0801-6
- Heirman, G., Vandewalle, L., Van Gemert, D., Wallevik, Ó., 2008. Integration approach of the Couette inverse problem of powder type self-compacting concrete in a wide-gap concentric cylinder rheometer. *Journal of Non-Newtonian Fluid Mechanics* 150, 93-103. doi: 10.1016/j.jnnfm.2007.10.003
- Hitomi, J., Murai, Y., Park, H.J., Tasaka, Y., 2017. Ultrasound Flow-Monitoring and Flow-Metering of Air–Oil–Water Three-Layer Pipe Flows. *IEEE Access* 5, 15021-15029. doi: 10.1109/access.2017.2724300
- Hitomi, J., Nomura, S., Murai, Y., De Cesare, G., Tasaka, Y., Takeda, Y., Park, H.J., Sakaguchi, H., 2020. Measurement of the inner structure of turbidity currents by ultrasound velocity profiling. *Int. J. Multiphase Flow* 136, 103540. doi: <https://doi.org/10.1016/j.ijmultiphaseflow.2020.103540>

- Huang, S., Xie, C., Lenn, C., Yang, W., Wu, Z., 2013. Issues of a Combination of Ultrasonic Doppler Velocity Measurement with a Venturi for Multiphase Flow Metering, SPE Middle East Oil and Gas Show and Conference. Society of Petroleum Engineers, Manama, Bahrain, p. SPE 164442.10.2118/164442-MS
- Hurther, D., Lemmin, U., 1998. A constant-beam-width transducer for 3D acoustic Doppler profile measurements in open-channel flows. *Meas. Sci. Technol.* 9, 1706-1714. doi: 10.1088/0957-0233/9/10/010
- Kikura, H., Aritomi, M., Taishi, T., 2002. Effect of the measurement volume in turbulent pipe flow measurement by the ultrasonic velocity profile method (mean velocity profile and Reynolds stress measurement). *Exp. Fluids* 32, 188-196. doi: 10.1007/s003480100299
- Kikura, H., Murakawa, H., Aritomi, M., 2009. Velocity Profile Measurements in Bubbly Flow Using Multi-Wave Ultrasound Technique. *Chem. Eng. Commun.* 197, 114-133. doi: 10.1080/00986440902935705
- Kotzé, R., Haldenwang, R., Fester, V., Rössle, W., 2015. In-line rheological characterisation of wastewater sludges using non-invasive ultrasound sensor technology. *Water SA* 41. doi: 10.4314/wsa.v41i5.11
- Kotze, R., Wiklund, J., Haldenwang, R., 2013. Optimisation of Pulsed Ultrasonic Velocimetry system and transducer technology for industrial applications. *Ultrasonics* 53, 459-469. doi: 10.1016/j.ultras.2012.08.014
- Kotzé, R., Wiklund, J., Haldenwang, R., 2016. Application of ultrasound Doppler technique for in-line rheological characterization and flow visualization of concentrated suspensions. *The Canadian Journal of Chemical Engineering* 94, 1066-1075. doi: 10.1002/cjce.22486
- Kotzé, R., Wiklund, J., Haldenwang, R., Fester, V., 2011. Measurement and analysis of flow behaviour in complex geometries using the Ultrasonic Velocity Profiling (UVP) technique. *Flow. Meas. Instrum.* 22, 110-119. doi: 10.1016/j.flowmeasinst.2010.12.010
- Kouame, D., Girault, J.-M., Patat, F., 2003a. High Resolution Processing Techniques for Ultrasound Doppler Velocimetry in the Presence of Colored Noise. Part I: Nonstationary Methods. *IEEE Transactions on Ultrasonics Ferroelectrics and Frequency Control* 50, 257-266. doi: 10.1109/TUFFC.2003.1193620
- Kouame, D., Girault, J.M., Remenieras, J.P., Chemla, J.P., Lethiecq, M., 2003b. High resolution processing techniques for ultrasound doppler velocimetry in the presence of colored noise. Part II: Multiplephase pipe-flow velocity measurement. *IEEE Trans Ultrason Ferroelectr Freq Control* 50, 267-278. doi: 10.1109/tuffc.2003.1193620
- Kumara, W.A.S., Elseth, G., Halvorsen, B.M., Melaaen, M.C., 2010. Comparison of Particle Image Velocimetry and Laser Doppler Anemometry measurement methods applied to the oil–water flow in horizontal pipe. *Flow. Meas. Instrum.* 21, 105-117. doi: <https://doi.org/10.1016/j.flowmeasinst.2010.01.005>
- Lee, T.H., Hanes, D.M., 1995. Direct inversion method to measure the concentration profile of suspended particles using backscattered sound. *J. Geophys. Res.* 100. doi: 10.1029/94jc03068
- Lehtikangas, O., Karhunen, K., Vauhkonen, M., 2016. Reconstruction of velocity fields in electromagnetic flow tomography. *Philos Trans A Math Phys Eng Sci* 374, 20150334. doi: 10.1098/rsta.2015.0334

- Liang, F., Fang, Z., Chen, J., Sun, S., 2016. Investigating the liquid film characteristics of gas–liquid swirling flow using ultrasound doppler velocimetry. *AIChE Journal* 63, 2348-2357. doi: 10.1002/aic.15570
- Liu, H., Tan, C., Li, Z., Bao, Y., Dong, F., 2021a. Ultrasound Phase Array Tomography for Biphasic Medium Distribution Imaging Using Synthetic Aperture Beam Scanning. *IEEE Trans. Instrum. Meas.* 70, 1-12. doi: 10.1109/tim.2021.3072692
- Liu, W., Tan, C., Dong, F., 2021b. Doppler spectrum analysis and flow pattern identification of oil-water two-phase flow using dual-modality sensor. *Flow. Meas. Instrum.* 77, 101861. doi: <https://doi.org/10.1016/j.flowmeasinst.2020.101861>
- Liu, W.L., Tan, C., Dong, X.X., Dong, F., Murai, Y., 2018. Dispersed Oil-Water Two-Phase Flow Measurement Based on Pulse-Wave Ultrasonic Doppler Coupled With Electrical Sensors. *IEEE Trans. Instrum. Meas.* 67, 2129-2142. doi: 10.1109/tim.2018.2814069
- Longo, S., 2006. The effects of air bubbles on ultrasound velocity measurements. *Exp. Fluids* 41, 593-602. doi: 10.1007/s00348-006-0183-0
- Lucas, G.P., Zhao, X., 2013. Large probe arrays for measuring mean and time dependent local oil volume fraction and local oil velocity component distributions in inclined oil-in-water flows. *Flow. Meas. Instrum.* 32, 76-83. doi: <https://doi.org/10.1016/j.flowmeasinst.2013.04.003>
- Lynnworth, L.C., Liu, Y., 2006. Ultrasonic flowmeters: half-century progress report, 1955-2005. *Ultrasonics* 44 Suppl 1, e1371-1378. doi: 10.1016/j.ultras.2006.05.046
- Mader, K., Nauber, R., Galindo, V., Beyer, H., Buttner, L., Eckert, S., Czarske, J., 2017. Phased Array Ultrasound System for Planar Flow Mapping in Liquid Metals. *IEEE Trans Ultrason Ferroelectr Freq Control* 64, 1327-1335. doi: 10.1109/TUFFC.2017.2693920
- Mahadeva, D.V., Huang, S.M., Oddie, G., Baker, R.C., 2010. Study of the effect of beam spreading on systematic Doppler flow measurement errors, 2010 IEEE International Ultrasonics Symposium, pp. 711-714. doi: 10.1109/ultsym.2010.5935748
- Masala, T., Harvel, G., Chang, J.S., 2007. Separated two-phase flow regime parameter measurement by a high speed ultrasonic pulse-echo system. *Rev. Sci. Instrum.* 78, 114901. doi: 10.1063/1.2804117
- Matikainen, L., Irons, G.A., Morala, E., Chang, J.S., 1986. Ultrasonic system for the detection of transient liquid/gas interfaces using the pulse - echo technique. *Rev. Sci. Instrum.* 57, 1661-1666. doi: 10.1063/1.1138546
- Morriss, S.L., Hill, A.D., 1991. Measurement of Velocity Profiles in Upwards OilWater Flow Using Ultrasonic Doppler Velocimetry, 66th Annual Technical Conference and Exhibition of the Society of Petroleum Engineers. SPE, Dallas, TX, USA
- Morriss, S.L., Hill, A.D., 1993. Ultrasonic Imaging and Velocimetry in Two-Phase Pipe Flow. *Journal of Energy Resources Technology* 115, 108-116. doi: 10.1115/1.2905977

- Munkhbat, B., Ari, H., Hiroshige, K., 2018. Velocity Measurement on Two-phase Air Bubble Column Flow Using Array Ultrasonic Velocity Profiler. *International Journal of Computational Methods and Experimental Measurements* 6, 86-97. doi: 10.2495/CMEM-V6-N1-86-97
- Murai, Y., Fujii, H., Tasaka, Y., Takeda, Y., 2006. Turbulent Bubbly Channel Flow Investigated by Ultrasound Velocity Profiler. *Journal of Fluid Science and Technology* 1, 12-23. doi: 10.1299/jfst.1.12
- Murai, Y., Ohta, S., Shigetomi, A., Tasaka, Y., Takeda, Y., 2009. Development of an ultrasonic void fraction profiler. *Meas. Sci. Technol.* 20, 114003. doi: 10.1088/0957-0233/20/11/114003
- Murai, Y., Tasaka, Y., Nambu, Y., Takeda, Y., Gonzalez A, S.R., 2010. Ultrasonic detection of moving interfaces in gas–liquid two-phase flow. *Flow. Meas. Instrum.* 21, 356-366. doi: 10.1016/j.flowmeasinst.2010.03.007
- Murakawa, H., Ichimura, S., Sugimoto, K., Asano, H., Umezawa, S., Sugita, K., 2020. Evaluation method of transit time difference for clamp-on ultrasonic flowmeters in two-phase flows. *Exp. Therm Fluid Sci.* 112. doi: 10.1016/j.expthermflusci.2019.109957
- Murakawa, H., Kikura, H., Aritomi, M., 2003. Measurement of Liquid Turbulent Structure in Bubbly Flow at Low Void Fraction Using Ultrasonic Doppler Method. *J. Nucl. Sci. Technol.* 40, 644-654. doi: 10.1080/18811248.2003.9715402
- Murakawa, H., Kikura, H., Aritomi, M., 2005. Application of ultrasonic doppler method for bubbly flow measurement using two ultrasonic frequencies. *Exp. Therm Fluid Sci.* 29, 843-850. doi: 10.1016/j.expthermflusci.2005.03.002
- Murakawa, H., Kikura, H., Aritomi, M., 2008. Application of ultrasonic multi-wave method for two-phase bubbly and slug flows. *Flow. Meas. Instrum.* 19, 205-213. doi: 10.1016/j.flowmeasinst.2007.06.010
- Murakawa, H., Muramatsu, E., Sugimoto, K., Takenaka, N., Furuichi, N., 2015. A dealiasing method for use with ultrasonic pulsed Doppler in measuring velocity profiles and flow rates in pipes. *Meas. Sci. Technol.* 26, 085301. doi: 10.1088/0957-0233/26/8/085301
- Muramatsu, E., Murakawa, H., Hashiguchi, D., Sugimoto, K., Asano, H., Wada, S., Furuichi, N., 2018. Applicability of hybrid ultrasonic flow meter for wide-range flow-rate under distorted velocity profile conditions. *Exp. Therm Fluid Sci.* 94, 49-58. doi: 10.1016/j.expthermflusci.2018.01.032
- Na, G., Park, J.-H., Jo, H., Jo, D., 2021. Measuring void fraction in vertical air–water bubbly flow using echo intensity and visualization techniques. *Prog. Nuclear Energy* 136. doi: 10.1016/j.pnucene.2021.103731
- Nabavi, M., Siddiqui, K., 2010. A critical review on advanced velocity measurement techniques in pulsating flows. *Meas. Sci. Technol.* 21, 042002. doi: 10.1088/0957-0233/21/4/042002
- Nauber, R., Buttner, L., Eckert, K., Frohlich, J., Czarske, J., Heitkam, S., 2018. Ultrasonic measurements of the bulk flow field in foams. *Phys Rev E* 97, 013113. doi: 10.1103/PhysRevE.97.013113
- Nguyen, T.T., Kikura, H., Duong, N.H., Murakawa, H., Tsuzuki, N., 2013a. Measurements of single-phase and

two-phase flows in a vertical pipe using ultrasonic pulse Doppler method and ultrasonic time-domain cross-correlation method. *Vietnam Journal of Mechanics* 35, 239-256. doi:

Nguyen, T.T., Murakawa, H., Tsuzuki, N., Duong, H.N., Kikura, H., 2016a. Ultrasonic Doppler Velocity Profile Measurement of Single-and Two-Phase Flows Using Spike Excitation. *Experimental Techniques* 40, 1235-1248. doi: 10.1007/s40799-016-0123-8

Nguyen, T.T., Murakawa, H., Tsuzuki, N., Kikura, H., 2013b. Development of Multiwave Method Using Ultrasonic Pulse Doppler Method for Measuring Two-phase Flow. *Journal of the Japanese Society for Experimental Mechanics* 13, 277-284. doi: 10.11395/jjsem.13.277

Nguyen, T.T., Tsuzuki, N., Murakawa, H., Duong, N.H., Kikura, H., 2016b. Measurement of the condensation rate of vapor bubbles rising upward in subcooled water by using two ultrasonic frequencies. *Int. J. Heat Mass Transfer* 99, 159-169. doi: 10.1016/j.ijheatmasstransfer.2016.03.109

Nnabuiife, S.G., Pilario, K.E.S., Lao, L., Cao, Y., Shafiee, M., 2019. Identification of gas-liquid flow regimes using a non-intrusive Doppler ultrasonic sensor and virtual flow regime maps. *Flow. Meas. Instrum.* 68, 101568. doi: 10.1016/j.flowmeasinst.2019.05.002

Obayashi, H., Tasaka, Y., Kon, S., Takeda, Y., 2008. Velocity vector profile measurement using multiple ultrasonic transducers. *Flow. Meas. Instrum.* 19, 189-195. doi: 10.1016/j.flowmeasinst.2007.11.007

Ouriev, B., Windhab, E., 2002. Rheological study of concentrated suspensions in pressure-driven shear flow using a novel in-line ultrasound Doppler method. *Exp. Fluids* 32, 204-211. doi: 10.1007/s003480100345

Park, H.J., Akasaka, S., Tasaka, Y., Murai, Y., 2021. Monitoring of Void Fraction and Bubble Size in Narrow-channel Bubbly-flows using Ultrasonic Pulses with A Super Bubble-resonant Frequency. *IEEE Sens. J.* 21, 273-283. doi: 10.1109/JSEN.2020.3015132

Park, H.J., Tasaka, Y., Murai, Y., 2015. Ultrasonic pulse echography for bubbles traveling in the proximity of a wall. *Meas. Sci. Technol.* 26, 125301. doi: 10.1088/0957-0233/26/12/125301

Park, J.-R., Chun, M.-H., 1985. Liquid Film Thickness Measurement by An Ultrasonic Pulse Echo Method. *Journal of the Korean Nuclear Society* 17, 25-33. doi:

Plesset, M.S., Prosperetti, A., 1977. Bubble Dynamics and Cavitation. *Annual Review of Fluid Mechanics* 9, 145-185. doi: 10.1146/annurev.fl.09.010177.001045

Poelma, C., 2016. Ultrasound Imaging Velocimetry: a review. *Exp. Fluids* 58. doi: 10.1007/s00348-016-2283-9

Povolny, A., Kikura, H., Ihara, T., 2018. Ultrasound Pulse-Echo Coupled with a Tracking Technique for Simultaneous Measurement of Multiple Bubbles. *Sensors (Basel)* 18, 1327. doi: 10.3390/s18051327

Prakash, B., Parmar, H., Shah, M.T., Pareek, V.K., Anthony, L., Utikar, R.P., 2019. Simultaneous measurements of two phases using an optical probe. *Experimental and Computational Multiphase Flow* 1, 233-241. doi: 10.1007/s42757-019-0025-y

- Ricci, S., Liard, M., Birkhofer, B., Lootens, D., Bruhwiler, A., Tortoli, P., 2012. Embedded Doppler system for industrial in-line rheometry. *IEEE Trans Ultrason Ferroelectr Freq Control* 59, 1395-1401. doi: 10.1109/TUFFC.2012.2340
- Ricci, S., Meacci, V., Birkhofer, B., Wiklund, J., 2017. FPGA-Based System for In-Line Measurement of Velocity Profiles of Fluids in Industrial Pipe Flow. *IEEE Trans. Ind. Electron.* 64, 3997-4005. doi: 10.1109/tie.2016.2645503
- Rolland, T., Lemmin, U., 1997. A two-component acoustic velocity profiler for use in turbulent open-channel flow. *Journal of Hydraulic Research* 35, 545-562. doi: 10.1080/00221689709498410
- Rusli, I.H., Aleksandrova, S., Medina, H., Benjamin, S.F., 2018. Using single-sensor hot-wire anemometry for velocity measurements in confined swirling flows. *Meas.* 129, 277-280. doi: <https://doi.org/10.1016/j.measurement.2018.07.024>
- Satomura, S., 1957. Ultrasonic Doppler Method for the Inspection of Cardiac Functions. *The Journal of the Acoustical Society of America* 29, 1181-1185. doi: 10.1121/1.1908737
- Satomura, S., 1959. Study of the flow patterns in peripheral arteries by ultrasonics. *Journal of the Acoustical Society of Japan* 15, 151–158. doi: 10.20697/jasj.15.3_151
- Scarano, F., 2013. Tomographic PIV: principles and practice. *Meas. Sci. Technol.* 24, 012001. doi: 10.1088/0957-0233/24/1/012001
- Shaban, H., Tavoularis, S., 2014. Identification of flow regime in vertical upward air–water pipe flow using differential pressure signals and elastic maps. *Int. J. Multiphase Flow* 61, 62-72. doi: <https://doi.org/10.1016/j.ijmultiphaseflow.2014.01.009>
- Shi, X., Tan, C., Dong, F., Murai, Y., 2019. Oil-gas-water three-phase flow characterization and velocity measurement based on time-frequency decomposition. *Int. J. Multiphase Flow* 111, 219-231. doi: 10.1016/j.ijmultiphaseflow.2018.11.006
- Shi, X.W., Tan, C., Dong, X.X., Dong, F., 2018. Structural Velocity Measurement of Gas-Liquid Slug Flow Based on EMD of Continuous Wave Ultrasonic. *IEEE Trans. Instrum. Meas.* 67, 2662-2675. doi: 10.1109/tim.2018.2826858
- Shi, X.W., Tan, C., Wu, H., Dong, F., 2021. An Electrical and Ultrasonic Doppler System for Industrial Multiphase Flow Measurement. *IEEE Trans. Instrum. Meas.* 70, 9154454. doi: 10.1109/tim.2020.3013080
- Shiratori, T., Tasaka, Y., Oishi, Y., Murai, Y., 2015. Ultrasonic velocity profiling rheometry based on a widened circular Couette flow. *Meas. Sci. Technol.* 26, 085302. doi: 10.1088/0957-0233/26/8/085302
- Shwin, S., Hamdani, A., Takahashi, H., Kikura, H., 2017. Experimental Investigation of Two-Dimensional Velocity on the 90° Double Bend Pipe Flow Using Ultrasound Technique. *World Journal of Mechanics* 07, 340-359. doi: 10.4236/wjm.2017.712026
- Supardan, M., Masuda, Y., Maezawa, A., Uchida, S., 2007. The investigation of gas holdup distribution in a

- two-phase bubble column using ultrasonic computed tomography. *Chem. Eng. J.* 130, 125-133. doi: 10.1016/j.cej.2006.08.035
- Suzuki, Y., Nakagawa, M., Aritomi, M., Murakawa, H., Kikura, H., Mori, M., 2002. Microstructure of the flow field around a bubble in counter-current bubbly flow. *Exp. Therm Fluid Sci.* 26, 221-227. doi:
- Takeda, Y., 1986. Velocity profile measurement by ultrasound Doppler shift method. *Int. J. Heat Fluid Flow* 7, 313-318. doi:
- Takeda, Y., 1987. Measurement of Velocity Profile of Mercury Flow by Ultrasound Doppler Shift Method. *Nucl. Technol.* 79, 120-124. doi: 10.13182/nt87-a16010
- Takeda, Y., 1991. Development of an ultrasound velocity profile monitor. *Nucl. Eng. Des.* 126, 277-284. doi:
- Takeda, Y., 1995. Instantaneous Velocity Profile Measurement by Ultrasonic Doppler Method. *JSME International Journal Series B* 38, 8-16. doi: 10.1299/jsmeb.38.8
- Takeda, Y., 2012. *Ultrasonic Doppler Velocity Profiler for Fluid Flow*. Springer, Tokyo, Japan.
- Tan, C., Dong, X.X., Dong, F., 2018. Continuous Wave Ultrasonic Doppler Modeling for Oil-Gas-Water Three-Phase Flow Velocity Measurement. *IEEE Sens. J.* 18, 3703-3713. doi: 10.1109/jsen.2018.2812834
- Tan, C., Li, X., Liu, H., Dong, F., 2019. An Ultrasonic Transmission/Reflection Tomography System for Industrial Multiphase Flow Imaging. *IEEE Trans. Ind. Electron.* 66, 9539-9548. doi: 10.1109/tie.2019.2891455
- Tan, C., Wu, H., Dong, F., 2013. Mass Flow Rate Measurement of Oil-Water Two-Phase Flow by a Long-Waist Cone Meter. *IEEE Trans. Instrum. Meas.* 62, 2795-2804. doi: 10.1109/tim.2013.2263660
- Tan, C., Yuan, Y., Dong, X., Dong, F., 2016. Oil-water two-phase flow measurement with combined ultrasonic transducer and electrical sensors. *Meas. Sci. Technol.* 27, 125307. doi: 10.1088/0957-0233/27/12/125307
- Tasaka, Y., Kimura, T., Murai, Y., 2014. Estimating the effective viscosity of bubble suspensions in oscillatory shear flows by means of ultrasonic spinning rheometry. *Exp. Fluids* 56, 1867. doi: 10.1007/s00348-014-1867-5
- Tasaka, Y., Yoshida, T., Rapberger, R., Murai, Y., 2018. Linear viscoelastic analysis using frequency-domain algorithm on oscillating circular shear flows for bubble suspensions. *Rheol. Acta* 57, 229-240. doi: 10.1007/s00397-018-1074-z
- Thorn, R., Johansen, G.A., Hjertaker, B.T., 2013. Three-phase flow measurement in the petroleum industry. *Meas. Sci. Technol.* 24, 012003. doi: 10.1088/0957-0233/24/1/012003
- Treenuson, W., Tsuzuki, N., Kikura, H., Aritomi, M., Wada, S., Tezuka, K., 2013. Accurate Flowrate Measurement on the Double Bent Pipe using Ultrasonic Velocity Profile Method. *Journal of the Japanese Society for Experimental Mechanics* 13, 200-211. doi: 10.11395/jjsem.13.200
- Turpeinen, T., Jäsberg, A., Haavisto, S., Liukkonen, J., Salmela, J., Koponen, A.I., 2020. Pipe rheology of microfibrillated cellulose suspensions. *Cellulose* 27, 141-156. doi: 10.1007/s10570-019-02784-4

- Wada, S., Kikura, H., Aritomi, M., 2006. Pattern recognition and signal processing of ultrasonic echo signal on two-phase flow. *Flow. Meas. Instrum.* 17, 207-224. doi: 10.1016/j.flowmeasinst.2005.11.006
- Wada, S., Kikura, H., Aritomi, M., Mori, M., Takeda, Y., 2004. Development of Pulse Ultrasonic Doppler Method for Flow Rate Measurement in Power Plant Multilines Flow Rate Measurement on Metal Pipe. *J. Nucl. Sci. Technol.* 41, 339-346. doi: 10.1080/18811248.2004.9715493
- Wang, S.-Q., Xu, K.-W., Kim, H.-B., 2020. Slug flow identification using ultrasound Doppler velocimetry. *Int. J. Heat Mass Transfer* 148, 119004. doi: 10.1016/j.ijheatmasstransfer.2019.119004
- Wang, T., Wang, J., Ren, F., Jin, Y., 2003. Application of Doppler ultrasound velocimetry in multiphase flow. *Chem. Eng. J.* 92, 111-122. doi: 10.1016/s1385-8947(02)00128-6
- Wang, Z.H., Wang, S.D., Meng, X., Ni, M.J., 2017. UDV measurements of single bubble rising in a liquid metal Galinstan with a transverse magnetic field. *Int. J. Multiphase Flow* 94, 201-208. doi: 10.1016/j.ijmultiphaseflow.2017.05.001
- Wiklund, J., Stading, M., 2008. Application of in-line ultrasound Doppler-based UVP–PD rheometry method to concentrated model and industrial suspensions. *Flow. Meas. Instrum.* 19, 171-179. doi: 10.1016/j.flowmeasinst.2007.11.002
- Wongsaroj, W., Hamdani, A., Thong-un, N., Takahashi, H., Kikura, H., 2017. Ultrasonic Measurement of Velocity Profile on Bubbly Flow Using Fast Fourier Transform (FFT) Technique. *IOP Conference Series: Materials Science and Engineering* 249, 012011. doi: 10.1088/1757-899x/249/1/012011
- Wongsaroj, W., Hamdani, A., Thong-un, N., Takahashi, H., Kikura, H., 2019. Extended Short-Time Fourier Transform for Ultrasonic Velocity Profiler on Two-Phase Bubbly Flow Using a Single Resonant Frequency. *Applied Sciences* 9, 50. doi: 10.3390/app9010050
- Wongsaroj, W., Owen, J.T., Takahashi, H., Thong-Un, N., Kikura, H., 2020. 2D velocity vector profile measurement on bubbly flow using ultrasonic technique. *Mechanical Engineering Journal* 7, 19-00519-00519-00519. doi: 10.1299/mej.19-00519
- Wunderlich, T., Brunn, P.O., 1999. Ultrasound pulse Doppler method as a viscometer for process monitoring. *Flow. Meas. Instrum.* 10, 201-205. doi: 10.1016/s0955-5986(99)00016-3
- Yan, Y., Wang, L., Wang, T., Wang, X., Hu, Y., Duan, Q., 2018. Application of soft computing techniques to multiphase flow measurement: A review. *Flow. Meas. Instrum.* 60, 30-43. doi: 10.1016/j.flowmeasinst.2018.02.017
- Yin, P., Cao, X., Li, Y., Yang, W., Bian, J., 2018. Experimental and numerical investigation on slug initiation and initial development behavior in hilly-terrain pipeline at a low superficial liquid velocity. *Int. J. Multiphase Flow* 101, 85-96. doi: 10.1016/j.ijmultiphaseflow.2018.01.004
- Yin, P., Cao, X., Zhang, P., Yang, W., Bian, J., Guo, D., 2020. Investigation of slug flow characteristics in hilly terrain pipeline using ultrasonic Doppler method. *Chem. Eng. Sci.* 211, 115300. doi: 10.1016/j.ces.2019.115300

Yoshida, T., Tasaka, Y., Murai, Y., 2017. Rheological evaluation of complex fluids using ultrasonic spinning rheometry in an open container. *J. Rheol.* 61, 537-549. doi: 10.1122/1.4980852

Yoshida, T., Tasaka, Y., Murai, Y., 2019. Efficacy assessments in ultrasonic spinning rheometry: Linear viscoelastic analysis on non-Newtonian fluids. *J. Rheol.* 63, 503-517. doi: 10.1122/1.5086986

Yu, H., Tan, C., Dong, F., 2021. Measurement of Particle Concentration by Multifrequency Ultrasound Attenuation in Liquid-Solid Dispersion. *IEEE Trans Ultrason Ferroelectr Freq Control* 68, 843-853. doi: 10.1109/TUFFC.2020.3020361

Zhai, L.S., Jin, N.D., Gao, Z.K., Zhao, A., Zhu, L., 2014. Cross-correlation velocity measurement of horizontal oil–water two-phase flow by using parallel–wire capacitance probe. *Exp. Therm Fluid Sci.* 53, 277-289. doi: <https://doi.org/10.1016/j.expthermflusci.2013.12.021>

Zhang, Y., Azman, A.N., Xu, K.-W., Kang, C., Kim, H.-B., 2020. Two-phase flow regime identification based on the liquid-phase velocity information and machine learning. *Exp. Fluids* 61. doi: 10.1007/s00348-020-03046-x

Zhou, S., Suzuki, Y., Aritomi, M., Matsuzaki, M., Takeda, Y., Mori, M., 1998. Measurement System of Bubbly Flow Using Ultrasonic Velocity Profile Monitor and Video Data Processing Unit, (III). *J. Nucl. Sci. Technol.* 35, 335-343. doi: 10.1080/18811248.1998.9733869